Metabolic Engineering 76 (2023) 179–192

Contents lists available at ScienceDirect

Metabolic Engineering

journal homepage: www.elsevier.com/locate/meteng

Laboratory evolution reveals general and specific tolerance mechanisms for commodity chemicals

Rebecca M. Lennen [a,1], Hyun Gyu Lim [b,1], Kristian Jensen [a,1], Elsayed T. Mohammed [a], Patrick V. Phaneuf [a], Myung Hyun Noh [b], Sailesh Malla [a], Rosa A. Börner [a], Ksenia Chekina [a], Emre Özdemir [a], Ida Bonde [a], Anna Koza [a], Jérôme Maury [a], Lasse E. Pedersen [a], Lars Y. Schöning [a], Nikolaus Sonnenschein [a], Bernhard O. Palsson [a,b], Alex T. Nielsen [a], Morten O.A. Sommer [a], Markus J. Herrgård [a,c,**], Adam M. Feist [a,b,*]

[a] The Novo Nordisk Foundation Center for Biosustainability, Technical University of Denmark, Building 220, Kemitorvet, 2800, Kgs. Lyngby, Denmark
[b] Department of Bioengineering, University of California, San Diego, 9500 Gilman Dr. #0412, La Jolla, CA, 92093-0412, USA
[c] BioInnovation Institute, Ole Maaløes Vej 3, 2830, Copenhagen, Denmark

ARTICLE INFO

Keywords:
Adaptive laboratory evolution
Chemical tolerance
Osmotolerance
Biochemical production

ABSTRACT

Although strain tolerance to high product concentrations is a barrier to the economically viable biomanufacturing of industrial chemicals, chemical tolerance mechanisms are often unknown. To reveal tolerance mechanisms, an automated platform was utilized to evolve *Escherichia coli* to grow optimally in the presence of 11 industrial chemicals (1,2-propanediol, 2,3-butanediol, glutarate, adipate, putrescine, hexamethylenediamine, butanol, isobutyrate, coumarate, octanoate, hexanoate), reaching tolerance at concentrations 60%–400% higher than initial toxic levels. Sequencing genomes of 223 isolates from 89 populations, reverse engineering, and cross-compound tolerance profiling were employed to uncover tolerance mechanisms. We show that: 1) cells are tolerized via frequent mutation of membrane transporters or cell wall-associated proteins (e.g., ProV, KgtP, SapB, NagA, NagC, MreB), transcription and translation machineries (e.g., RpoA, RpoB, RpoC, RpsA, RpsG, NusA, Rho), stress signaling proteins (e.g., RelA, SspA, SpoT, YobF), and for certain chemicals, regulators and enzymes in metabolism (e.g., MetJ, NadR, GudD, PurT); 2) osmotic stress plays a significant role in tolerance when chemical concentrations exceed a general threshold and mutated genes frequently overlap with those enabling chemical tolerance in membrane transporters and cell wall-associated proteins; 3) tolerization to a specific chemical generally improves tolerance to structurally similar compounds whereas a tradeoff can occur on dissimilar chemicals, and 4) using pre-tolerized starting isolates can hugely enhance the subsequent production of chemicals when a production pathway is inserted in many, but not all, evolved tolerized host strains, underpinning the need for evolving multiple parallel populations. Taken as a whole, this study provides a comprehensive genotype-phenotype map based on identified mutations and growth phenotypes for 223 chemical tolerant isolates.

1. Introduction

Despite advances in synthetic and systems biology tools to engineer and study metabolism, developing microbial strains for commercial-level chemical production remains a significant challenge (Mohedano et al., 2022; Van Dien, 2013; Wehrs et al., 2019). The stressful conditions that production strains encounter in large-scale industrial processes are one of the most critical hurdles for achieving commercialization (Deparis et al., 2017; Wehrs et al., 2019). High concentrations of the desired compound are one of the major stresses present in industrial production conditions (Mukhopadhyay, 2015; Wehrs et al., 2019). Such chemical stresses can have inhibitory effects on host organisms, which

* Co-corresponding author. The Novo Nordisk Foundation Center for Biosustainability, Technical University of Denmark, Building 220, Kemitorvet, 2800, Kgs. Lyngby, Denmark.
** Corresponding author. BioInnovation Institute, Ole Maaløes Vej 3, 2830, Copenhagen, Denmark.
E-mail addresses: mjh@bii.dk (M.J. Herrgård), afeist@biosustain.dtu.dk (A.M. Feist).
[1] These authors contributed equally to the work.

https://doi.org/10.1016/j.ymben.2023.01.012
Received 11 October 2022; Received in revised form 6 January 2023; Accepted 30 January 2023
Available online 3 February 2023

limit achievable titers without employing product removal strategies.

High levels of products decrease cellular viability by adversely affecting diverse essential functions (e.g., DNA replication, energy generation, membrane maintenance), and related mechanisms vary greatly depending on the chemical species. Lack of knowledge about the molecular mechanisms of chemical toxicity or tolerance makes rational engineering of tolerant phenotypes challenging (Lim et al., 2020; Qi et al., 2019). Such challenges in tolerance engineering can result in choosing a more robust (Thorwall et al., 2020) but potentially otherwise difficult to engineer production organism, or alternatively using non-rational approaches to engineer tolerance. These approaches include induced random mutagenesis or screening (Kim et al., 2021), transcription factor engineering (Alper et al., 2006), and adaptive laboratory evolution (ALE) (Anand et al., 2019; Du et al., 2020; Sandberg et al., 2019). In particular, the ALE strategy has been successfully employed to obtain strains that tolerate product chemicals (Kildegaard et al., 2014; Mundhada et al., 2017; Qi et al., 2019; Sandberg et al., 2019; Yomano et al., 1998).

Although the ALE strategy has been vigorously applied to investigate tolerance mechanisms (Mans et al., 2018; Sandberg et al., 2019; Wu et al., 2022), most studies focused on a single target chemical of interest and/or characterized one or few isolates from a single evolved population. Thus, identified mechanisms are likely chemical-specific and isolate- or population-specific. In addition, product tolerized ALE isolates have, in some cases, shown an increased production of the target chemicals (Mundhada et al., 2017; Nguyen-Vo et al., 2019; Pereira et al., 2019; Radi et al., 2022; Royce et al., 2015), whereas in other cases no significant improvement in production has been observed (Atsumi et al., 2010; Kildegaard et al., 2014). Beyond the understanding of individual chemical tolerance, efforts to characterize broad chemical resistance have been undertaken (Nyabako et al., 2020; Pham et al., 2017). For example, isolates tolerant to acidic pH could be successfully secured through ALE (Du et al., 2020; Harden et al., 2015), and they displayed increased tolerance to a broad range of acids, but it was difficult to ascertain the mechanism via mutational analysis. Thus, additional work is needed to understand tolerance to a broader range of chemicals, including organic acids, for example. Such data can serve as an important cornerstone for elucidating the key principles for chemical tolerance of microorganisms. Furthermore, identified beneficial mutations can be utilized to improve production of a broad spectrum of target chemicals.

Here, we applied a systematic automated ALE approach to elucidate general and specific mechanisms of chemical tolerance in *Escherichia coli*. We chose eleven chemicals belonging to six different functional groups and tolerized *E. coli* K-12 MG1655 (MG1655) against them: two diols - 1,2-propanediol (12PD) and 2,3-butanediol (23BD); two diamines - hexamethylenediamine (HDMA) and putrescine (PUTR); two diacids - glutarate (GLUT) and adipate (ADIP); two fatty acids - hexanoate (HEXA) and octanoate (OCTA); and other organic acids and one alcohol - isobutyrate (IBUA), *p*-coumarate (COUM), and *n*-butanol (BUT). Systematic genomic and phenotypic analyses of 223 evolved isolates then allowed for the determination of general features of chemical tolerance. We further demonstrated the utility of testing isolates from multiple parallel-evolved populations by testing the endogenous production of two chemicals, 23BD and IBUA, across a large number of isolates as background strains. It was established that evolving for tolerance can greatly improve production, although the degree of improvement depends on the specific genotype of the evolved isolate. Collectively, we believe that our study provides a comprehensive reference dataset for future engineering efforts for improving biochemicals. All sequencing results of isolates tolerized for individual chemicals are publicly available at ALEdb (https://aledb.org/).

2. Materials and methods

2.1. Strains and media

MG1655 was used as the starting strain for the ALE experiments and as the reference strain for all subsequent characterization. Chemicals were purchased from Sigma-Aldrich (St. Louis, MO), Fisher Scientific (Waltham, MA), or TCI (TCI Europe N.V., Zwijndrecht, Belgium) unless otherwise specified. Plasmids for IBUA and 23BD production were generously donated by authors (Xu et al., 2014; Zhang et al., 2011).

For all cell cultures, M9 glucose medium supplemented with 10 g/L glucose was formulated with 10x M9 salts, 2 mM $MgSO_4$, 100 μM $CaCl_2$ and 1x trace elements. A stock solution of 10x M9 salts consisted of 68 g/L Na_2HPO_4, 30 g/L KH_2PO_4, 5 g/L NaCl, and 10 g/L NH_4Cl. 2000x M9 Trace element stock solution contained 3.0 g/L $FeSO_4{\cdot}7H_2O$, 4.5 g/L $ZnSO_4{\cdot}7H_2O$, 0.3 g/L $CoCl_2{\cdot}6H_2O$, 0.4 g/L $Na_2MoO_4{\cdot}2H_2O$, 4.5 g/L $CaCl_2{\cdot}H_2O$, 0.2 g/L $CuSO_4{\cdot}2H_2O$, 1.0 g/L H_3BO_3, 15 g/L disodium EDTA, 0.1 g/L KI, 0.7 g/L $MnCl_2{\cdot}4H_2O$. All medium and stock solutions were prepared by using Milli-Q filtered water and autoclaved or filtered. All laboratory evolutions, screening and cultivation experiments were performed at pH 7.0 with neutralization by adding NaOH when needed. Diamines were purchased as hydrochloric acid salts, and 23BD was a 98% mixture of racemic and *meso* forms (Acros Organics, Geel, Belgium).

2.2. Adaptive laboratory evolution for tolerization

The toxicity of each of the chemicals was tested by screening growth of MG1655 in different concentrations (Fig. S1). Three biological replicates of MG1655 were cultivated at 37 °C with 250 rpm shaking in 10 mL of the M9 medium in 50 mL Falcon tubes. Cells were grown to mid-exponential phase and back-diluted to OD_{600} (optical density at 600 nm) 0.05 in 1.4 mL of the glucose M9 medium with the chosen chemicals at different concentrations at pH 7 in 48-well flower plates. The cultures were then incubated in a BioLector microbioreactor system (m2p-labs GmbH, Baesweiler, Germany) at 37 °C with 1000 rpm shaking. Initial concentrations for ALE were chosen so that MG1655 could obtain a growth rate of approximately 0.4 h^{-1}. The initial and final evolution concentrations, as well as the screening concentrations for all the chosen chemicals are shown in Table S1.

ALE was performed with gradually increasing concentrations of each chemical in glucose M9 medium. The growth medium adjusted to pH 7.0 to ensure an evolutionary pressure for tolerating the specific chemical compounds rather than tolerance towards low or high pH. Cells were serially passaged during exponential growth for approximately 40 days using an automated liquid-handler platform (LaCroix et al., 2017). Cells were cultured at 37 °C with full aeration at 1200 rpm stirring speed. Once OD_{600} reached approximately 1.0, 150 μL was passed into a new tube with 15 mL fresh media containing the respective chemical concentration. Over the course of the experiment, cells were kept in the exponential growth phase in order to keep a constant selection pressure for growth rate. Machine outages or errors occasionally allowed cultures to enter the stationary phase. The OD_{600} was measured by a Sunrise Plate Reader (Tecan, Switzerland). Growth rates were determined by computing the slope of $\log(OD_{600})$ using linear regression with the Polyfit function in MATLAB developed by Mathworks (Natick, MA). When an increase in the apparent growth rate was achieved (average growth rate for all of the parallel replicates) at a particular concentration that was maintained over more than one passage, the chemical concentration was increased. This process was repeated in cycles until an increase in tolerated concentration was achieved. In incidents where the increase in the chemical concentration caused cells to crash, i.e., cell death, chemical concentration was reduced to a level that allowed cell growth and cells were reinoculated from the last cryogenic stock that was taken or from recent stationary phase cultures still on the machine deck. Periodically, samples were frozen in 25% v/v glycerol and stored

at −80 °C for further use.

2.3. Primary tolerance screening

Populations from evolution endpoints were plated on LB agar plates (or on M9 agar for a few octanoic acid evolved populations due to growth not being observed on LB agar) and ten (or three for NaCl-tolerized populations) individual colonies from each population were screened for growth at the maximum concentration for which robust growth rates were achieved during the evolution (Table S1 and Fig. S2). Cultures of the wildtype strain, *E. coli* K-12 MG1655, were used as controls. The isolates were inoculated in 300 μL of glucose M9 medium in deep-well plates and incubated in a wide-throw shaker at 37 °C and 300 rpm. The next day, cells were diluted 10X in a fresh medium and 30 μL was transferred to clear-bottomed square 96 well half-deepwell plates (EnzyScreen, Heemstede, Netherlands) containing 270 μL M9 + glucose supplemented with the corresponding toxic chemical at concentrations as in Table S1 at pH 7.0 (isolate screening concentration). The plates were incubated at 37 °C with 225 RPM shaking in a Growth Profiler screening platform from EnzyScreen BV (Heemstede, Netherlands). The green pixel values were converted to OD_{600} values using a previously established calibration curve for K-12 MG1655. The resulting growth curves for all 890 isolates were inspected qualitatively for isolates exhibiting robust growth as assessed by lag time and growth rate as compared to K-12 MG1655 controls. Each of the 10 isolates per population from the primary screening were grouped according to close similarities based on the above criteria. For most populations, isolates representative of each group were picked for further analysis (typically 2–3 isolates per population), for a total of 20 isolates per chemical (24 isolates for GLUT). Secondary growth screening of all isolates in 3 biological replicates was performed in 48-well FlowerPlates (m2p-labs, Baesweiler, Germany) using a BioLector microbioreactor system, as previously described (Lennen and Herrgård, 2014).

2.4. Whole-genome sequencing

Whole-genome sequencing libraries of tolerized isolates against the eleven chemicals were generated using the TruSeq^R Nano DNA LT Library Prep Kit (Illumina, San Diego, CA). Briefly, 100 ng of genomic DNA diluted in 52.5 μL TE buffer was fragmented in Covaris Crimp Cap microtubes on a Covaris E220 ultrasonicator (Woburn, MA) with 5% duty factor, 175 W peak incident power, 200 cycles/burst, and 50 s duration under frequency sweeping mode at 5.5–6 °C (Illumina recommendations for a 350-bp average fragment size). The ends of fragmented DNA were repaired by T4 DNA polymerase, Klenow DNA polymerase, and T4 polynucleotide kinase. The Klenow exo minus enzyme was then used to add an 'A' base to the 3′ end of the DNA fragments. The adapters were ligated to the ends of the DNA fragments, and the DNA fragments ranging from 300 to 400 bp were recovered by beads purification. Finally, the adapter-modified DNA fragments were enriched by 3 cycle PCR. The final concentration of each library was measured on a Qubit^R 2.0 Fluorometer using the Qubit DNA Broad range assay kit (Life Technologies). Average dsDNA library size was determined using the Agilent DNA 7500 kit on an Agilent 2100 Bioanalyzer. Libraries were sequenced by using a MiSeq Reagent kit v2 (300 cycles, illumina) on a MiSeq platform with a paired-end protocol and read lengths of 151 bases. For isolates tolerized against NaCl, genomic DNA libraries were prepared by using a a plexWell™ 96 kit (seqWell, Beverly, MA) according to the manufacturer's protocol and similarly sequenced but using a NovaSeq 6000 platform (300 cycles, Illumina).

2.5. Mutation data analysis

Raw sequencing reads were analyzed with the Breseq pipeline (Deatherage and Barrick, 2014) through the ALEdb platform (Phaneuf et al., 2019) to generate lists of mutations for each evolved isolate. The genome sequence for MG1655 with the Genbank accession number NC_000913.3 was used as a reference. Each mutation was mapped to a corresponding gene; intragenic mutations were mapped to any gene whose coding sequence overlapped with the mutation; intergenic mutations were mapped to a closer gene coding region from the mutation. Preexisting mutations in the MG1655 strain were taken from a previous study (LaCroix et al., 2015), and were confirmed to be identical to those in the previous study by resequencing cells from the same cryogenic stock in other studies on-site.

2.6. Growth curve data analysis

The growth curves generated by the instruments were processed using the *croissance* python package (http://github.com/biosustain/croissance) to obtain growth rates (See **Supplementary Note 1** for details). Cell growth was monitored and quantified from OD_{600} for the Growth Profiler, or light backscatter intensities for growth curves obtained with the BioLector. For each growth rate, a normalized growth rate was calculated by subtracting the mean growth rate of the wildtype strain, MG1655, on the same plate and in the same medium. This procedure was done to remove the effects of any between-plate and between-experiment growth variations.

2.7. Cross-tolerance screening

Cells were inoculated into 300 μL of the glucose M9 medium in 96 deep well plates in biological triplicates (except for five biological replicates for MG1655) and the cultures were incubated at 37 °C and 300 rpm overnight. The next day, 30 μL of the cultures was added to 270 μL of the same fresh medium supplemented with chemicals at pH 7.0 in a 96 well plate format, and the plates were incubated in a Growth Profiler (EnzyScreen BV) at 37 °C and 225 rpm. The medium was supplemented with a corresponding chemical (Table S1). Cross-tolerance screening was performed at lower levels of chemicals than those for primary ALE isolate screening to allow the wild type strain to grow in all conditions.

2.8. Genome editing of MG1655

Strains containing the relevant single gene deletions were obtained from the Keio Collection and were transduced via P1*vir* phage into the MG1655 background strain using a protocol previously described (Lennen et al., 2011), or via Lambda Red recombineering using pSIM5 as previously described (Datta et al., 2006; Lennen and Herrgård, 2014), with confirmation of deletions made by colony PCR. Site directed changes in the *E. coli* genome of evolved strains were made using two cycles of ssDNA-mediated recombineering using a previously described protocol (Lennen et al., 2016). Mutants were identified using a colony qPCR assay where a shift in cycle threshold values could be observed between a wildtype control and positive hits using a primer specific to the desired mutant at the 3′ end, plus an additional destabilizing mutation at the −3 position from the 3′ end. Identified mutants were confirmed by Sanger sequencing.

2.9. IBUA and 23BD production

To produce IBUA, *yqhD* was deleted from each of the isolates evolved on isobutyrate to reduce the conversion of isobutyrate to isobutanol. The strains were then transformed with pIBA1 (harboring *ilvD* from *E. coli* and *alsS* from *Bacillus subtilis*) and pIBA7 (harboring *kivD* encoding 2-ketoacid decarboxylase from *Lactococcus lactis* and *padA,* now named *feaB,* encoding phenylacetaldehyde dehydrogenase from *E. coli*) plasmids (Zhang et al., 2011) and precultured into 300 μL of LB media supplemented with kanamycin (50 μg/mL) and ampicillin (100 μg/mL) in 96 deep well plate and incubated at 37 °C with 300 rpm overnight in quadruplicates. *E. coli* K-12 MG1655 Δ*yqhD*/pIBA1/pIBA7 was used as a control. The following day, 24 μL of pre-inoculum was transferred into

2.4 mL of two-times diluted FIT medium (discontinued Feed-in-Time Medium from m2p-labs, Baesweiler, Germany) with 200 mM MOPS, supplemented with antibiotics. Then the culture plates were incubated at 30 °C and 300 RPM. After 6 h of incubation, 100 μM of IPTG was added to the media and further incubated at 30 °C and 300 rpm.

To produce 23BD, the pET-RABC plasmid containing a 23BD gene cluster (*lysR-budABC*) from *Enterobacter cloacae* subsp. *dissolvens* SDM (Xu et al., 2014) were introduced into the wildtype or evolved strains that had deletions of *hsdR*, encoding one subunit of the endogenous EcoKI restriction enzyme. This was necessary to enable transformation of pET-RABC, which harbors an EcoKI restriction site. The strains were transformed with pET-RABC and precultured in 300 μL of M9 + glucose supplemented with 5 g/L yeast extract and kanamycin (50 μg/mL) in a 96 deep well plate and incubated at 37 °C with 300 rpm overnight in quadruplicates. MG1655 Δ*hsdR*/pET-RABC was used as a control. The following day, 20 μL of pre-inoculum was transferred into 2 mL of the same medium in 24 deep well plates and incubated at 30 °C and 300 rpm.

The amounts of IBUA or 23BD were quantified by HPLC (Ultimate 3000, Thermo Scientific, USA) with an Aminex^{R} HPX-87H ion exclusion column (300 mm × 7.8 mm, Bio-Rad Laboratories, Denmark) connected to a refractive index detector and a UV detector (205 nm, 210 nm, 254 nm and 280 nm). An isocratic elution with flow rate of 0.5 mL min^{-1} of 5 mM sulfuric acid was used for 30 min. Under these conditions, IBUA was detected under the 210 nm UV channel at a retention time of 20.3 min, and stereoisomers of 23BD were detected under the RI detector channel at the retention times of 17.4 min and 18.3 min. Using the peak area, the total amount of IBUA was calculated. For absolute quantification, a calibration curve was drawn using 0.5, 1, 2.5, 4, 5, 7.5 10, and 12.5 g/L concentrations ($y = 35.487x - 2.3142$, $R^2 = 0.9993$) for IBUA and 1, 5, 10, 12.5, 15 and 25 g/L concentrations ($y = 6.5119x + 0.5464$, $R^2 = 0.9999$) for 23BD.

3. Results and discussion

3.1. ALE improved tolerance of E. coli against the eleven chemicals

To understand chemical tolerance mechanisms in *E. coli*, we employed a systematic workflow (Fig. 1a) which included automated serial passaging with increased concentrations of targeted chemicals (Fig. 1b and Table S2) for tolerization, growth phenotyping, mutation analysis, reverse engineering, and endogenous production testing. These eleven chemicals represent diverse chemical classes with commercial potential (Erian et al., 2018; Fedorchuk et al., 2020; Henritzi et al., 2018; Jendresen et al., 2015; Lim et al., 2015; Niu et al., 2019; Noh et al., 2017; Park et al., 2013; Pontrelli et al., 2018; Qian et al., 2009; Volker et al., 2014; Wu et al., 2018; Xu et al., 2014; Zhang et al., 2011; Zhao et al., 2018) and different initial levels of toxicity (Fig. S1); diols, diacids, and diamines inhibited cell growth when their concentrations reached greater than 10 g/L whereas growth inhibition by the other chemicals (i.e., "fatty acids" and "others" classes) occurred at concentrations below 5 g/L in the tested condition. Growth inhibition by chemicals in the same classes were similar. A few ALE studies were previously performed for improving tolerance of *E. coli* against OCTA (Chen et al., 2020; Royce et al., 2015) and BUT (Horinouchi et al., 2017; Reyes et al., 2012, 2013; Zorraquino et al., 2017) and results from those studies served as direct comparisons (**Supplementary Note 2**). Efforts to engineer microorganisms for improved production have been previously undertaken for all of the compounds, thus indicating their importance to bioproduction (Table S2).

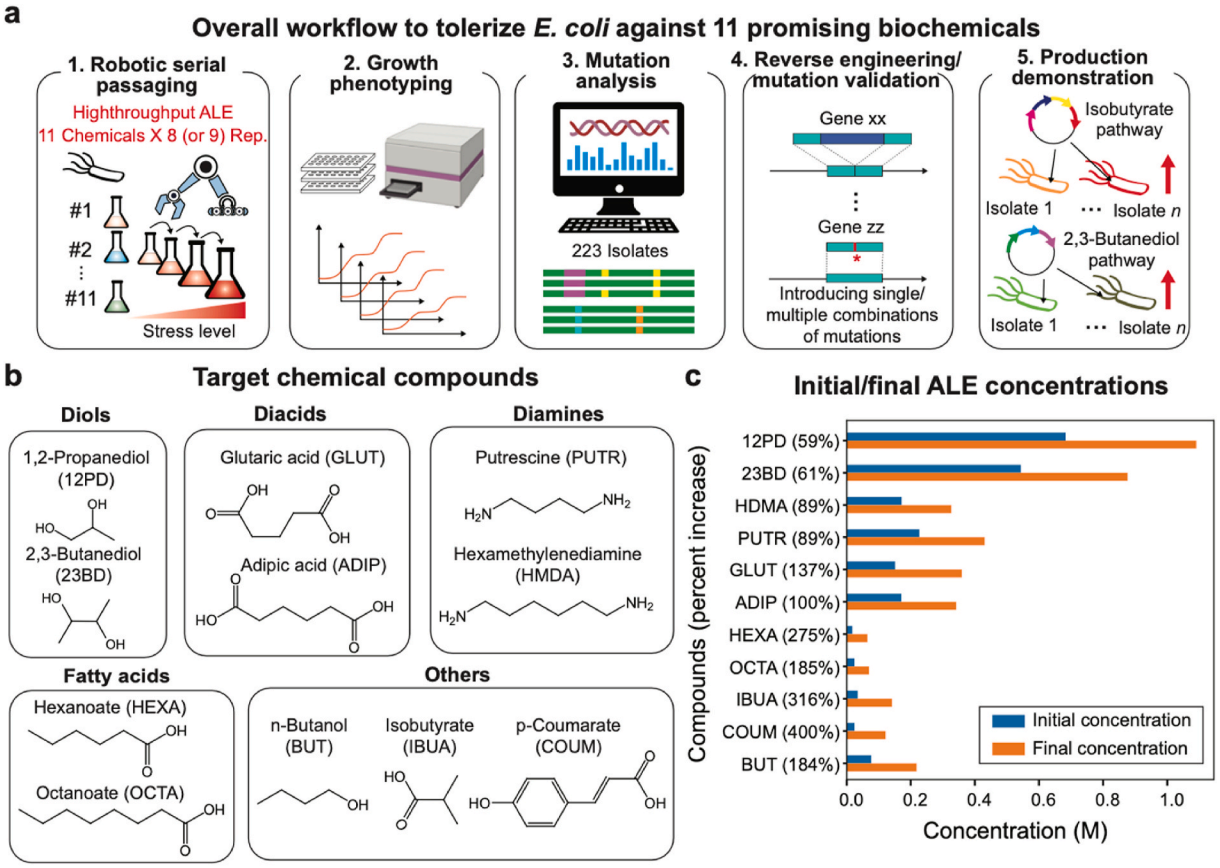

Fig. 1. Overview of tolerization ALE experiments against 11 promising biochemicals
(**a**) Overall workflow of the study. (**b**) 11 target chemicals selected for the study grouped by chemical category. (**c**) Initial and final molar concentrations of the chemicals used during ALE and the percentage increases, in parentheses, in tolerated concentration.

An automated serial passage platform was utilized to evolve eight independent populations (nine for BUT) of MG1655 to tolerate toxic levels of each chemical, resulting in a total of 89 independently evolved populations all starting from the same initial genotype. Chemical concentrations were increased in a stepwise manner over approximately 800 generations per individual replicate for a given compound; the concentrations reached substantially higher levels (60%–400% of the starting concentrations, Fig. 1c) while maintaining robust growth of populations (i.e., growth rate $>0.2\ h^{-1}$). None of the evolved populations exhibited detectable growth within a reasonable timeframe (i.e., approx. 1 week) with a target chemical as a sole carbon source in M9 agar plates without glucose, indicating that they had not evolved the ability to degrade the compound to an extent to support the growth rate improvements observed (data not shown). More than twenty randomly chosen isolates from each of the final flasks for each population were then screened for the ability to grow in the final stressed concentration (or slightly reduced for COUM, HEXA, and OCTA evolved isolates, Table S1) of a chemical, and up to three isolates per population that grew robustly were selected for further characterization. Notably, 202 isolates out the total analyzed 223 isolates (>90%) showed largely increased growth rates in the presence of a corresponding chemical, compared to those of the wildtype strain (Fig. S2), indicating that the ALE strategy effectively improved tolerance to each chemical. This set of the 223 isolates was subjected to further characterization and engineering using the systematic workflow (Fig. 1a).

3.2. Comparative mutation analysis reveals key genetic regions associated with improved chemical tolerance and suggests diverse tolerance mechanisms

To identify mutations present in the tolerant strains, all down-selected isolates were subjected to whole-genome sequencing (Fig. 2 and see details in the **Methods** section). After a preliminary analysis, 31 out of the 223 isolates were excluded from the further analysis (**Supplementary Dataset**) since they had mutations in mismatch repair system genes (i.e., *mutS, mutT, mutY, mutL*) that resulted in a hypermutator phenotype (Horst et al., 1999). In the 192 isolates, a total of 930 mutations affecting 367 genes were identified; the median number of sequence variants in the isolates was six (Fig. 2a).

To identify key tolerance mechanisms, we focused on genes mutated in at least four independent lineages, regardless of the target chemicals (Fig. 2b–d and Table S3). With these criteria, a total of 36 genes were found to be commonly mutated in the evolved isolates. These genes hosted a wide range of unique mutations, ranging from very little (e.g., a single mutation, T128S, in *nanK*) to a large variety of unique mutations (e.g., 43 unique mutations in *rpoA*, *rpoB*, *rpoC* encoding RNA polymerase subunits, Fig. S3). We found some mutations which were previously reported; for example, H419P in *rpoC* in OCTA-tolerized isolates was reported previously in the same condition (Chen et al., 2020). In addition, at least one loss-of-function (LoF) mutation (i.e., premature stop codon termination, frameshift, or mobile element insertion) was observed in 101 genes, which corresponded to 27.5% of the total identified mutated genes, indicating LoF of a gene played an important role in altering cellular phenotypes. The large variety of mutations suggested that they could have different effects on their hosts, although evidence also exists suggesting that mutations to the same gene from one or multiple selection pressures may converge on the same functional effect (e.g., LoF from different experiments) on the gene (Peng et al., 2018; Phaneuf et al., 2021).

We further categorized the 36 genes which were common mutation targets depending on the number of observed ALE conditions (i.e., chemicals) into three different groups: 6 culturing-condition adaptation genes whose mutations were previously-reported in an identical non-stressor ALE condition (i.e., a control) (LaCroix et al., 2015), 19 general tolerance genes which were mutated in ALE conditions for multiple chemical classes, and 11 chemical-specific tolerance genes which were mutated in isolates tolerized against chemicals in the same class (except the "others" class). The six culturing-condition adaptation genes (Fig. 2b and Table S3) include: (1) *pyrE* encoding orotate phosphoribosyltransferase, (2) *rpoB* encoding RNA polymerase (RNAP) subunit β, (3) *hns* encoding DNA-binding transcriptional dual regulator H-NS, (4) *yeaR* encoding a hypothetical protein, (5) *pykF* encoding pyruvate kinase 1, and (6) *mreB* encoding dynamic cell cytoskeletal protein MreB. Some of these genes were also mutated in other previous *E. coli* ALE studies (Conrad et al., 2010; Wang et al., 2018) where conditions were unrelated to the 11 chemicals. Consequently, some of the mutations, especially when they are the same ones observed in other conditions, may not be related to improved chemical tolerance but rather could have allowed better fitness in M9 glucose medium (LaCroix et al., 2015). Treating this set as a control condition for fast growth in the culturing condition, we primarily focused on the other 30 genes (Fig. 2c) and inferred tolerance mechanisms based on reported functions of the tolerance-related genes and mutation types (Fig. 3 and **Supplementary Information**).

General tolerance genes were determined and categorized (Fig. 2b and Table S3). Specifically, the 19 genes for general tolerance were responsible for five cellular functions (in the order of gene numbers): (1) six transporter genes (three importer-encoding genes: *proV* encoding glycine betaine ABC transporter ATP binding subunit, *pstS* encoding phosphate ABC transporter periplasmic binding protein, and *manY* encoding mannose-specific PTS enzyme IIC component; and three exporter-encoding or related regulatory genes: *sapB* encoding putrescine ABC exporter membrane subunit SapB, *mprA* encoding DNA-binding transcriptional repressor MprA, and *mdtK* encoding multidrug efflux pump MdtK), (2) six transcription/translation machinery genes (*rpoC* encoding RNAP subunit β′, *rpoA* encoding RNAP subunit α, *rpsA* encoding 30S ribosomal subunit protein S1, *rnt* encoding RNase T, *rnb* encoding RNase II, *rho* encoding transcription termination factor Rho), and (3) five stress signaling genes (*spoT* encoding bifunctional (p)ppGpp synthase/hydrolase, *sspA* encoding stringent starvation protein A, *yobF* encoding DUF2527 domain-containing protein YobF, *barA* encoding sensor histidine kinase BarA, *cspC* encoding transcription antiterminator and regulator of mRNA stability CspC), and (4) two membrane component genes (*nagC* encoding DNA-binding transcriptional dual regulator NagC, *nagA* encoding N-acetylglucosamine-6-phosphate deacetylase, Figs. 2c and 3). It should be noted that *rho* was categorized to be a general tolerance gene because it was frequently mutated in the previous tolerization ALE study against BUT (Reyes et al., 2012), although this gene was only mutated in COUM-tolerized isolates in this study. These genes were independently mutated, on average, in four different ALE conditions (i.e., chemical conditions), implying that their mutations are not specific to a single chemical but broadly function for multiple chemicals.

Given their functions, it was inferred that general tolerance is achieved by alterations to the cell wall/membrane and transport across it, transcription and translation, and stress-related functional proteins. All of the above transport-encoding genes, except *sapB* and *manY*, acquired at least one clear LoF mutation, suggesting that expression of these genes is not beneficial to tolerance. Interestingly, mutations in some genes showed a trend in which seven genes: *proV*, *nagC, nagA*, *spoT*, *rpsA*, *rnt*, and *sspA,* were mostly mutated in isolates tolerized against the diols (12PD and 23BD), diacids (PUTR and GLUT), and diamines (ADIP and HDMA) with relatively high endpoint concentrations (i.e., osmolarities), whereas *sapB* (in addition to genes encoding other subunits of the SapBCDF putrescine exporter) was frequently mutated in isolates tolerized against fatty acids (OCTA and HEXA) and as well as other organic acids (COUM and IBUA) and BUT. This observation suggested that the level of osmotic stress of a medium significantly impacts chemical toxicity and related evolutionary tolerization mechanisms. Tolerance to all eleven chemicals was associated with at least three general stress genes, implying a substantial generality in tolerance mechanisms.

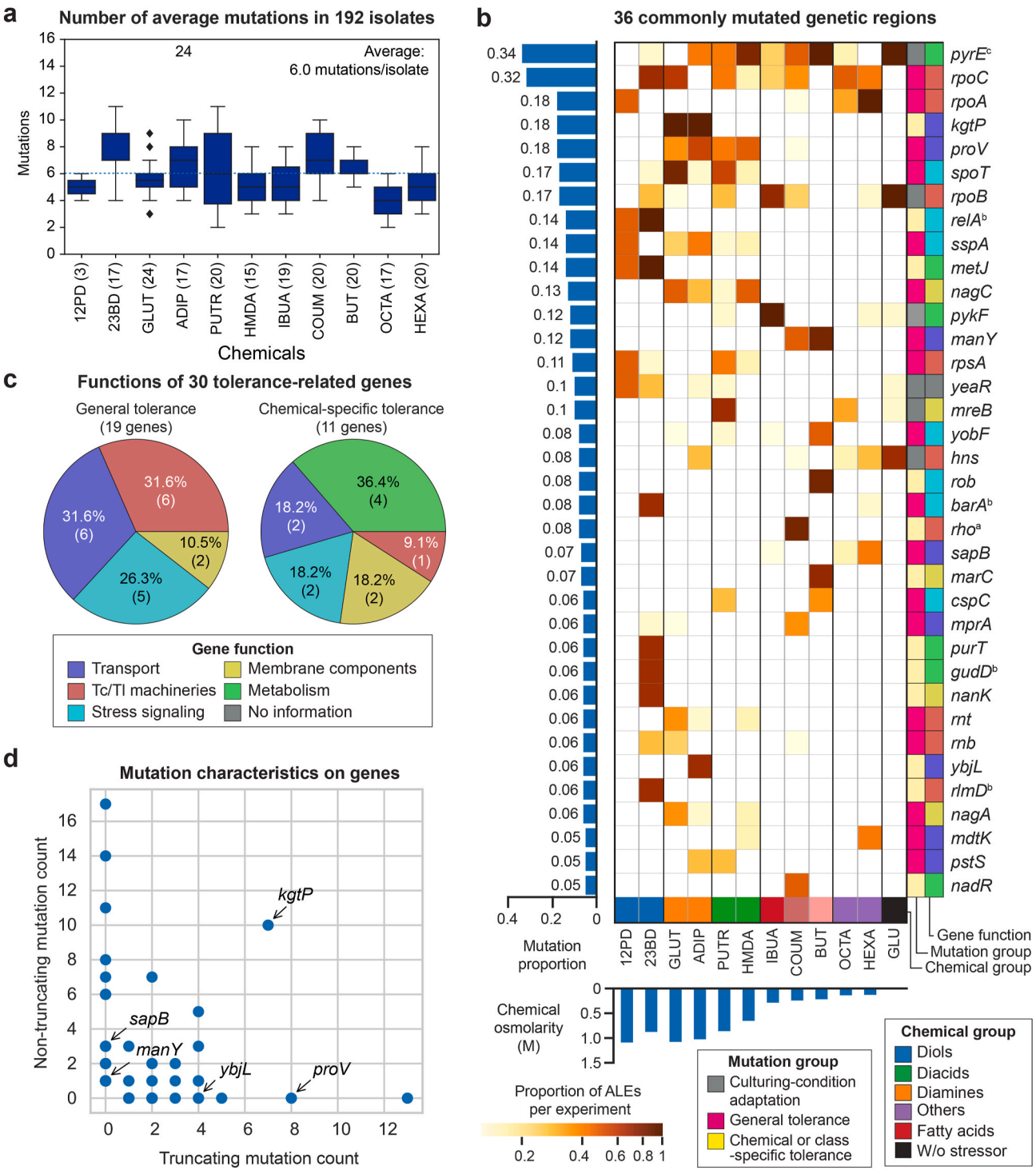

Fig. 2. Mutation analysis for tolerized isolates against 11 promising biochemicals

(**a**) Boxplots of the distributions of numbers of mutations per isolate for each condition (total number of isolates $n = 192$, hypermutators were excluded). Boxplots display the interquartile range (box), the median (line), and the full range of the data (whiskers), excluding outliers whose distance from the median is more than 1.5 times the interquartile range. The numbers above the boxes show the values of outliers not shown in the plots. The numbers in parentheses are the strain numbers in each group. (**b**) A frequency heatmap of 38 commonly mutated genes. The listed genes were mutated in four or more independent lineages across experimental conditions. Evolution conditions were listed in the order of chemical groups (the most bottom row colors) and the endpoint osmolarities as shown in the bottom bar blot. 'None' indicates the ALE condition without any stressors. The bottom left color bar shows proportions of isolates having mutations in a corresponding region out of the total sequenced isolates for each condition. The left bar plot shows the averaged proportion of ALE experiment where a corresponding gene was mutated for each condition. The two rightmost column colors show mutation groups and gene functions, respectively. [a]Although *rho* was mutated only in the COUM condition, it was categorized as general tolerance since its mutation was identified in a previous study that tolerized *E. coli* to BUT (Reyes et al., 2012). [b] denotes four adjacent genes (*relA, rlmD, barA, gudD*) removed by an identical Δ7,528 bp mutation that occurred in five independent ALEs. [c]Mutations in either *rph*, *pyrE*, or their intergenic region were counted together, given their known effect regarding the pyrimidine deficiency in *E. coli* K-12 strains (Jensen, 1993; LaCroix et al., 2015). (**c**) Functions of general and chemical-specific tolerance regions. Abbreviations: Tc, transcriptional; Tl, translation. (**d**) The count of observed non-truncating and truncating mutations for all mutated genetic features of this experiment. Raw data is available in **Supplementary Dataset**.

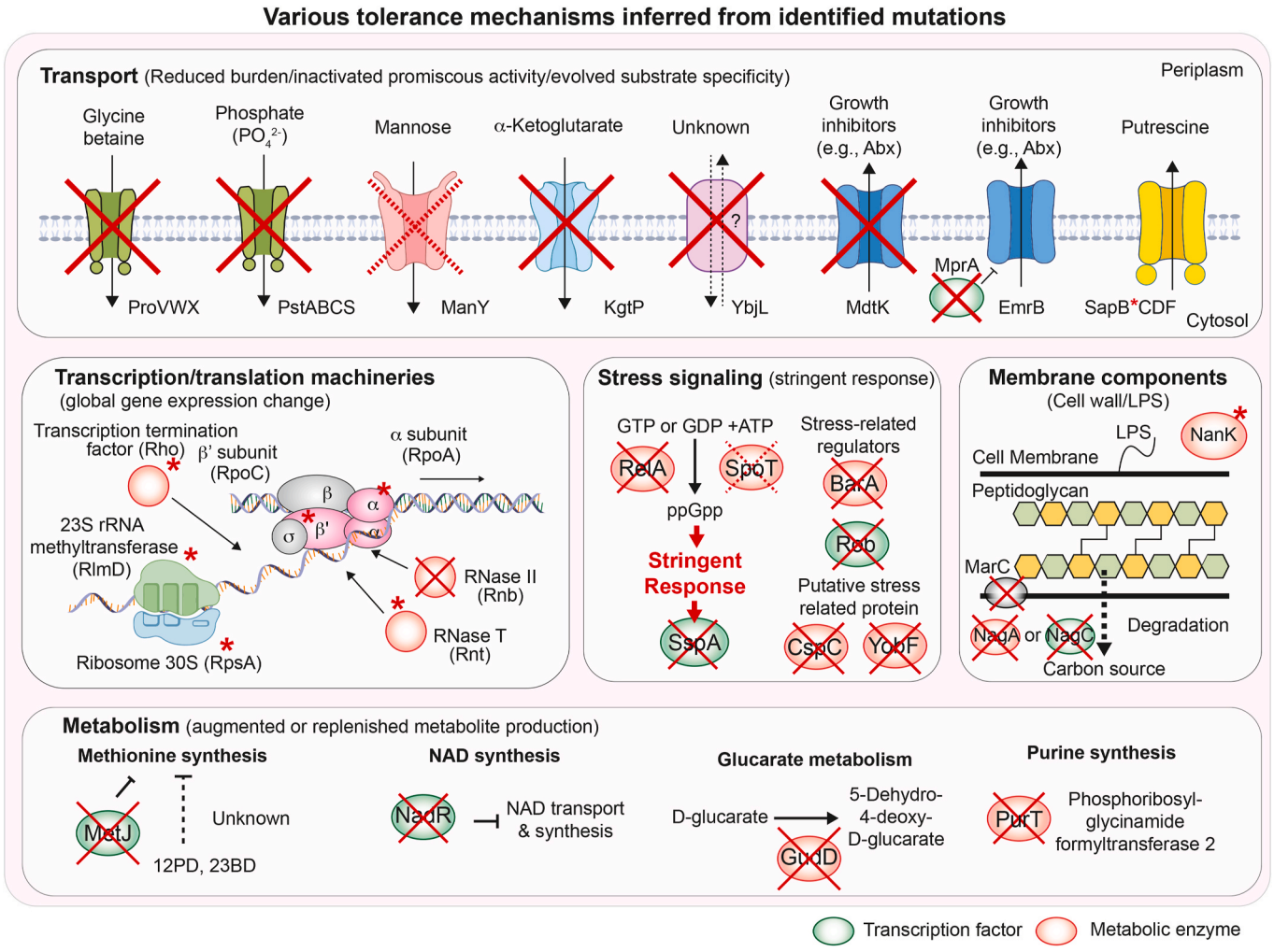

Fig. 3. Functions of mutated genes and inferred tolerance mechanisms

Diverse chemical tolerance mechanisms inferred from identified mutations in *E. coli*. Red 'Xs' indicate a gene acquired at least one truncation mutation likely resulting in LoF. '*' indicates genes only acquired non-truncation mutations (e.g., single amino acid changes). When no LoF mutations were observed but reduced activity was inferred based on their association to other similar genes (i.e., ManY, an importer; SpoT, ppGpp synthetase similar to RelA), dashed red lines were used for 'X'. *Transport*: LoF mutations (red 'X') were found in four importer-encoding genes (*proV*, *pstS*, *manY*, *kgtP*), one efflux-pump-encoding gene (*mdtK*), and one putative transporter gene (*ybjL*). Mutations in two efflux pump related genes (*mprA* and *sapB*) are likely augmenting export activity. *Transcription/translation machineries*: mutations were identified in genes encoding transcription or translation machineries such RNA polymerase subunits (*rpoA*, *rpoC*), transcription termination factor (*rho*), ribosome subunits (*rpsA*), and RNase (*rnb*, *rnt*). Given that most of these genes are critical for cells and acquired amino acid changes, it was inferred that gene expression was globally tuned for improved tolerance. *Stress signaling*: genes responsible for stringent response (e.g., *relA*, *spoT*, *sspA*) were inactivated by LoF mutations. *Membrane/cell wall components*: mutations were found in genes (*nagA*, *nagC, nanK*) related to catabolism of amino sugars such as N-glucosamine, key components of peptidoglycan or lipopolysaccharides for cell wall. *nagA* or *nagC* genes acquired LoF mutations whereas *nanK* acquired an identical single amino acid change mutation. *marC* also encodes an inner membrane protein; however, its function is unknown. *Metabolism*: genes related to metabolism of methionine and other cofactors (*metJ*), and NAD (*nadR*) were mutated likely to enhance their synthesis. Glucarate catabolism and purine biosynthesis genes were inactivated by LoF mutations in *gudD* and *purT*, indicating their expression is not beneficial for tolerance.

Genes that were targets of parallel evolution were also found to be specific to a given chemical or class, and we identified 11 such genes (Fig. 2b and Table S3). The greatest number of the genes were related to metabolism in this class (4 genes - *metJ* encoding DNA-binding transcriptional repressor for methionine biosynthesis, *nadR* encoding DNA-binding transcriptional repressor/nicotinamide mononucleotide adenylyltransferase NadR, *purT* encoding phosphoribosylglycinamide formyltransferase 2, and *gudD* encoding D-glucarate dehydratase). This observation was contrary to the fact that none of the general tolerance category genes were metabolism related genes. Other genes were responsible for stress signaling (*relA* encoding GDP/GTP pyrophosphokinase, *rob* encoding a DNA-binding transcriptional dual regulator Rob), transport (*kgtP* encoding α-ketoglutarate:H^+ symporter, *ybjL* encoding putative transport protein YbjL), transcription/translation machinery (*rlmD* encoding 23S rRNA m^5U1939 methyltransferase), and membrane components (*nanK* encoding N-acetylmannosamine kinase, *marC* encoding inner membrane protein MarC). Mutations in nine genes were specifically identified in only one chemical condition: BUT (*marC*, *rob*), 23BD (*nanK*, *gudD*, *purT*, *rlmD*), ADIP (*ybjL*), and COUM (*rho*, *nadR*). The other three genes were mutated in isolates from the same chemical class: diols (*relA*, *metJ*), and diacids (*kgtP*). The identification of individual chemical or chemical class-specific mutated genes with diverse functions implies a high diversity in mechanisms of toxicity and tolerance between the compounds, but also a similarity for chemicals within the same class. We inferred the specific tolerance mechanisms from the functions of mutated genes for each chemical (Fig. 3 and **Supplementary Note 2**). Out of all eleven chemical conditions examined, six (12PD, 23BD, GLUT, ADIP, COUM, BUT) had reproducible chemical and class-specific genes mutated. This finding indicates that for some chemicals, tolerance can be achieved through multiple non-convergent genotypes

in the evolved lineages which may have higher order connectivity (Phaneuf et al., 2020), in addition to general common mechanisms outlined previously.

3.3. Reverse engineering of commonly mutated genes validates their causality

We validated the causality of a number of mutated genes by reintroducing mutations into the wild-type strain via reverse engineering (Fig. 4 and Figs. S4a–k). We initially investigated genes that appeared to be very clear LoF mutations (Fig. 2d) due to, for example, frameshift mutations, insertions or deletions, or premature stop codons being present in at least one isolate while a range of other mutations were present in other populations evolved on the same chemical. As an example, for the broad LoF analysis, we chose three different transporter genes identified in GLUT (*kgtP*, *proV*) and ADIP-tolerant (*kgtP*, *proV*, *ybjL*) isolates. All isolates that were tolerized against diacids ($n = 41$ examined) contained mutations in *kgtP* (Fig. 2b); approximately half of these mutations were clearly LoF, i.e., frameshift mutations or single nucleotide polymorphisms (SNPs) that generated premature stop codons (Fig. 2d). Glutarate is structurally similar to α-ketoglutarate, the native substrate of KgtP, and this observation indicated glutarate import by KgtP was impaired. Indeed, growth on glutarate as a sole carbon source, which was observed to be possible for MG1655 over a span of weeks on M9 glutarate plates, no longer occurred or occurred very weakly in evolved isolates (Fig. S5). Similarly, many mutations in *proV* and *ybjL* were also clearly LoF. When we tested the deletions of these genes in MG1655, it was observed that the *kgtP* deletion strain grew much faster than the wildtype strain in high concentrations of the GLUT and ADIP (Fig. 4a and b). Sequential deletion of *proV* and *ybjL*, in addition to *kgtP*, further increased the growth rate on both of these diacids, with the triple deletion strain almost reaching the same growth rate on GLUT as the best evolved isolates. A possible reason why *ybjL* LoF mutations did not occur in any of the GLUT isolates is that other mutations that occurred in these strains, for example widespread SNPs in *spoT* that occurred in all isolates from 7 of 8 populations, were more beneficial. Collectively, it was concluded that the three genes are deleterious in the chemical-stressed condition.

We further interrogated a total of 52 additional genes mutated in sequenced isolates (**Supplementary Dataset**). These genes include 19 commonly mutated genes and an additional 33 genes that were either suspected to be LoF or were identified in other experiments to likely be causative in conditions where LoF mutations alone could not reconstitute the phenotype. Mutations were introduced as gene deletions in

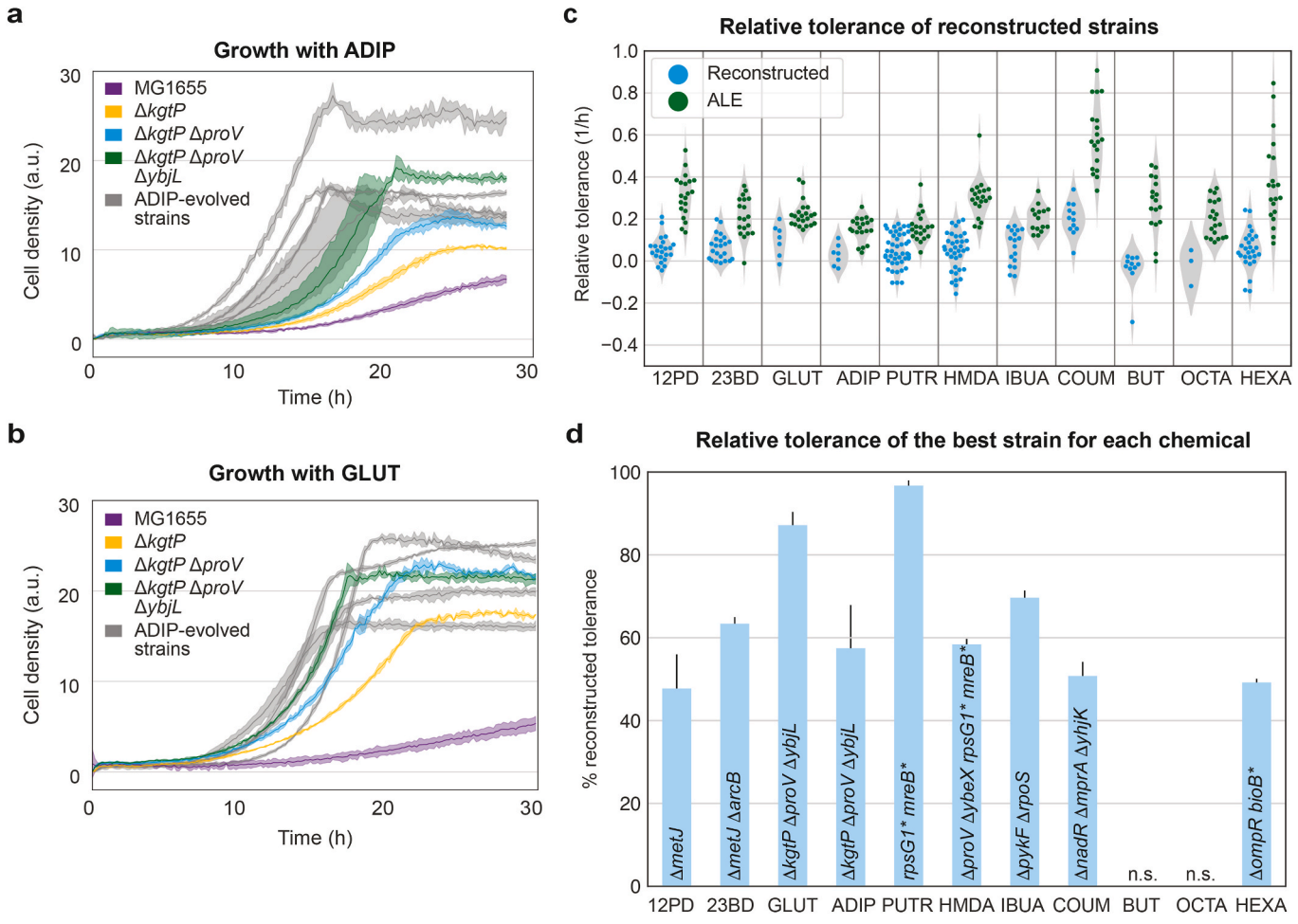

Fig. 4. Elucidation of causative mutations

(**a** and **b**) Growth curves of the reference strain MG1655, transporter deleted strains, and four evolved isolates tolerized against (**a**) ADIP and (**b**) GLUT in the presence of 50 g/L ADIP or 47.5 g/L GLUT. Lines show mean growth curves of three biological replicates, with error bars indicating the standard deviation about the mean. (**c**) Distributions of tolerance to each of the 11 chemicals for reconstructed strains and evolved isolates, respectively. Relative tolerance was defined as the growth rate in the presence of the given chemical relative to the growth rate of the wild type strain. Tolerance for each specific reconstructed strain is shown in Fig. S5. (**d**) The percentage of reconstructed tolerance to each of the chemicals, calculated as the relative tolerance of the best reconstructed strain divided by the 3rd quartile of relative tolerances of the evolved isolates. Error bars denote standard deviation of the growth rate of the reconstructed strain (biological replicates $n = 3$). n. s.:not significant. Reconstructed strains for BUT mostly showed reduced lag time (data not shown). See Table S3 for a list of reconstructed strain genotypes.

cases where the observed mutations were likely to result in LoF of the gene. For several essential genes (e.g., *rpoA*, *nusA*, *mreB*, *rpsG*, *spoT*), specific mutated SNPs were introduced to better reconstruct tolerance phenotypes for selected PUTR, HMDA, and COUM isolates. To validate causality of these genes, we generated a total of 140 genome-edited strains with single mutations (or their combinations) and evaluated their growth rates in the presence of relevant chemical stresses for each strain (Fig. 4a and Fig. S6). Notably, it was possible to reconstruct the tolerance to most of the chemicals, at least partially, by introducing up to four genome edits (Fig. 4d). In some cases, one or two edits can confer a great deal of tolerance, as has been previously reported (Anand et al., 2020; Lim et al., 2020; Radi et al., 2022). Other cases require higher combinations of edits. Nonetheless, these results confirmed the effects of reverse engineered genes in increased tolerance against the corresponding chemicals.

3.4. Evaluation of cross-chemical tolerance of evolved isolates

We evaluated the cross-chemical tolerance of 190 non-hypermutator isolates by growing them in the presence of moderately toxic levels of each of the 11 chemicals (Table S1). Two isolates from the original 192 had failed to grow in the minimal glucose medium precultures for unknown reasons and were not further examined. The growth rate difference between an isolate and the wildtype strain in a given condition was utilized as a measure of tolerance. To investigate their phenotypes in the absence of a chemical or with osmotic stressors for the counterions present when neutralizing the diamines or acids, these isolates were also grown in the base medium only or the base medium supplemented by NaCl at 0.6 M.

We found that isolates evolved on three pairs of similar compounds, i.e., diamines, diols and diacids, were generally tolerant to the other chemical of the same chemical class (Fig. 5a, upper 3 squares on diagonal). However, isolates tolerized against either OCTA or HEXA were not tolerant to the other fatty acid, although several genes (e.g., *rpoC*, *rpoA*, *sapB*) were commonly mutated (Fig. 5a, bottom square on diagonal). This observation suggested that mutations even in the same gene may result in different effects on chemical tolerance. For example, the H419P mutation in *rpoC* occurred in OCTA-tolerized isolates but most mutations in the same gene in HEXA-tolerized isolates were the P64L mutation (Supplementary Data); isolates from these two conditions did

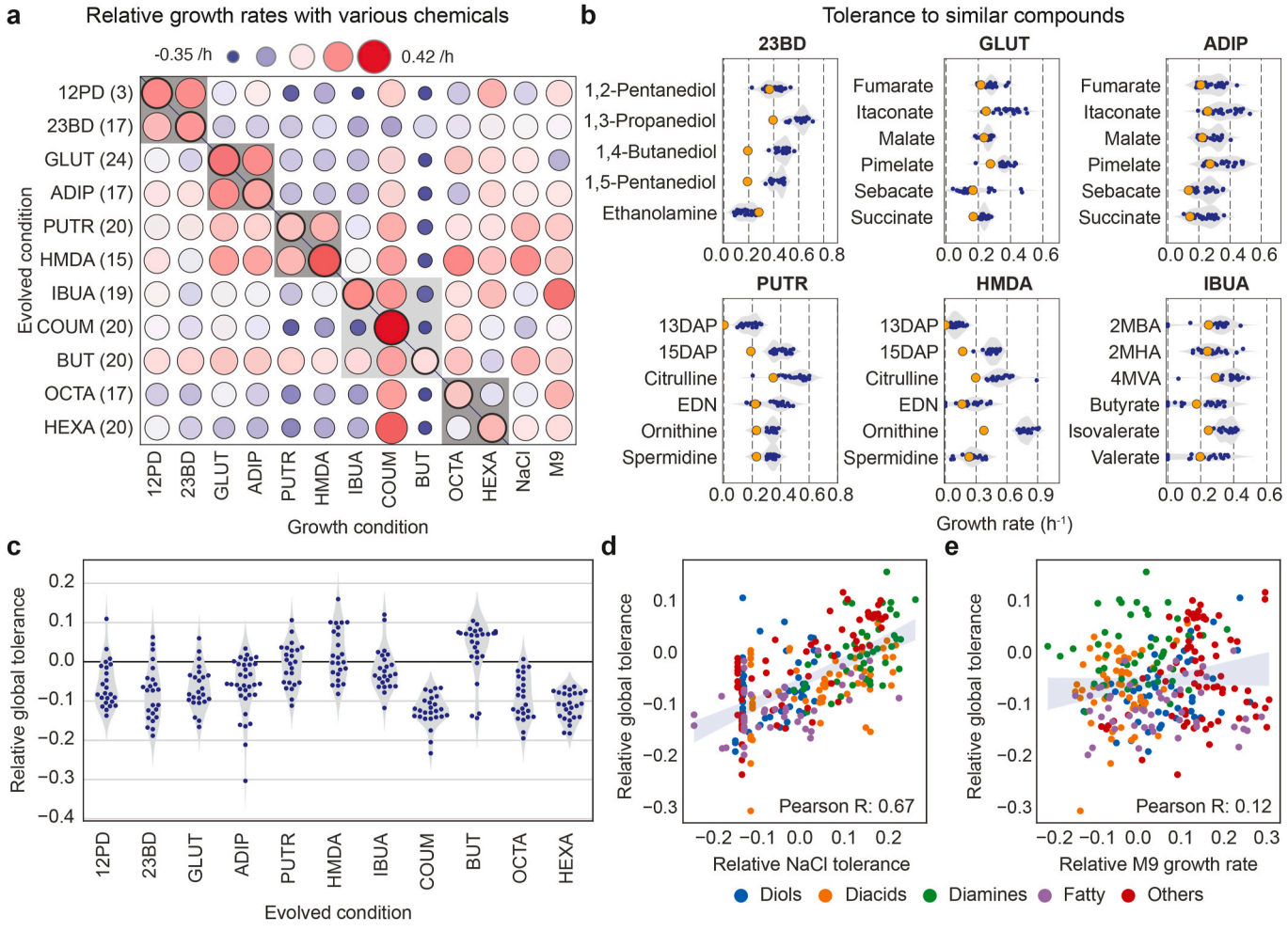

Fig. 5. Tolerance evaluation to the target chemicals for evolved isolates and other similar compounds.
(**a**) Cross-tolerance between the compounds used for ALE. Circle color and size represent the mean growth rate of the group of isolates relative to the unevolved reference strain (number of screened isolates in parenthesis and total $n = 190$). The gray boxes indicate pairs of compounds that are from a similar chemical class. The growth rates on M9 glucose +0.6 M NaCl and M9 glucose are also shown. (**b**) Isolates evolved in 23BD, GLUT, ADIP, PUTR, HMDA, and IBUA conditions were screened for tolerance against other chemically similar compounds that were not part of the set of ALE compounds. Blue points represent growth rates of evolved isolates, while the orange points show the growth rates of the wildtype strain. Concentration of each chemical is listed in **Supplementary Dataset** (**c**) Distribution of global tolerance values (i.e., average relative growth rate across all 11 chemicals) for isolates evolved on each of the 11 compounds. (**d**) Global tolerance as a function of osmotolerance (growth rate on M9 glucose + 0.6 M NaCl) and (**e**) as a function of improvement in baseline growth (growth on M9 glucose). Abbreviations: 13DAP, 1,3-diaminopropane; 15DAP, 1,5-diaminopentane; EDN, ethylenediamine; 2MBA, 2-methylbutyrate; 2MHA, 2-methylhexanoate; 4MVA, 4-methylvalerate.

not show cross-tolerance. Interestingly, the diamine-tolerized isolates were also mostly tolerant to the diacids, likely due to many commonly mutated genes (e.g., *spoT*, *proV*, *nagC*). Lastly, most tolerized isolates showed higher growth rates in an M9 medium without chemicals (Fig. 5a, far right column), likely due to mutations in genes for culturing-condition adaptation to fast growth (LaCroix et al., 2015). This finding highlights the approach of some ALE studies to first evolve to the media condition, then introduce a perturbation (McCloskey et al., 2018). Notably, the GLUT isolates showed a reduced growth rate on M9 with no stress, thus suggesting a possible tradeoff between resistance and an unstressed growth rate. In the analysis of convergent mutations (Fig. 2b), the expected results that the culture condition adaptations were not enriched in these clones is apparent.

Going beyond the set of 11 targeted chemicals from this study, we also tested whether isolates that were evolved on 23BD, GLUT, ADIP, PUTR, HMDA, and IBUA were tolerant to a broader range of similar compounds (Fig. 5b). Notably, we found that in most cases isolates tolerant to one compound also had improved growth rates on a wide range of similar compounds (although there were some exceptions, e.g., 23BD on ethanolamine, which is aminated). Increases in the averaged growth rate of the isolates tolerized against HDMA (0.21 h^{-1}) were higher than other isolates tolerized against 23BD (0.15 h^{-1}), ADIP (0.10 h^{-1}), and IBUA (0.07 h^{-1}). These results show that the enhanced tolerance functions for not only the targeted chemicals but also other structurally similar compounds, allowing their broad applicability.

We sought to understand the general features that make *E. coli* tolerant to a broad range of chemicals. We used the average growth rate of an ALE isolate relative to the wildtype strain across all 11 chemicals as a metric of global chemical tolerance of an isolate. This tolerance depended significantly on which chemical the specific isolate had been evolved to tolerate ($F = 10.06$, $p < 10^{-13}$, $n = 191$; Fig. 4c), and varied between isolates evolved to tolerate the same chemical (median standard deviation of 0.06 h^{-1}). Isolates evolved on HMDA typically had high global chemical tolerances whereas isolates evolved on COUM or HEXA were less tolerant to other chemicals compared to the wildtype strain. We found that NaCl tolerance was statistically significantly predictive of global chemical tolerance (Pearson's $r = 0.63$, $p < 10^{-33}$, $n = 281$; Fig. 4d). In contrast, the relative growth rate of a given ALE isolate in M9 glucose was not predictive of global chemical tolerance (Pearson's $r = 0.12$, $p = 0.04$, $n = 281$; Fig. 4e). The low correlation between M9 growth rate and global tolerance improvements is potentially due to a "fear-greed" tradeoff in a limited-resource environment (Anand et al., 2019; Sastry et al., 2019).

3.5. Tolerization to high salinity reveals genes mutated in response to osmotic stress

We hypothesized that osmotic stress played a major role in growth inhibition, and some genes were mutated in response to osmotic stress. Specifically, with a high concentration of an acidic or basic chemical, this stress could have been imposed by either a chemical itself or a salt ion (Na^+ or Cl^-) from an acid (HCl) or base (NaOH) that was used for neutralization. To test this hypothesis, we performed an additional ALE which tolerized *E. coli* to a high salinity generated by adding excess NaCl to the medium, with six replicates (see **Methods**, Fig. S7a). We were able to isolate evolved strains which showed improved fitness at 50 g/L of NaCl (~2 times higher osmolarity than the highest value in the chemical tolerization experiment, Fig. S7b). From a subsequent mutation analysis of evolved isolates, we found 14 common genes mutated in at least three isolates (**Supplementary Dataset**). Notably, at least one LoF mutation was observed in five general tolerance genes: *nagC, nagA*, *proV, mprA*, and *yobF* (Fig. 2b). Therefore, it is likely that these genes were mutated in response to increases in medium salinity and the deletions are beneficial (Fig. 4a and b). For example, the expression of *proV* was greatly upregulated under NaCl-induced stress (Fig. S8) even in the absence of its substrate, glycine betaine (Seo et al., 2017). Additionally, the commonality of mutation events in these genes across both high Na^+ and high Cl^- conditions may reflect a more general sensing mechanism of high osmolarity in *E. coli*. Indeed, a two-component histidine kinase/response regulator, EnvZ/OmpR, has been shown to generally sense osmolarity, independent of the chemical species (Wang et al., 2012). Collectively, these results indicate that increased salinity due to the presence of salt counterions imposed stress at high chemical concentrations examined in this study.

3.6. Improved production of IBUA and 23BD with tolerized isolates as hosts

To determine whether isolates evolved to tolerate high concentrations of a product could produce more of the corresponding product endogenously when used as a production strain background, production pathways were inserted into a set of ALE-derived isolates. We chose the two pyruvate-derived compounds, IBUA and 23BD, as examples since the two tolerized sets of isolates had very different genotypes and growth phenotypes (Figs. 2 and 5), and production of these compounds has previously been demonstrated in *E. coli* with minimal genomic modifications as well as plasmid-based heterologous gene expression (Xu et al., 2014; Yang and Zhang, 2019; Zhang et al., 2011).

We introduced an IBUA production pathway into wildtype MG1655 and 12 genetically distinct isobutyrate-tolerant isolates by expressing three heterologous genes (*alsS*, *kivD*, and *padA*) from plasmids (Zhang et al., 2011) and deleting a competing pathway gene (*yqhD*) in each isolate (Fig. 6a). The engineered ALE-derived strains had highly variable levels of production of IBUA, with 8 strains (66.7% of the tested strains) showing increased production of up to three-fold compared to the engineered wildtype strain (Fig. 6b), indicating that tolerance engineering is greatly advantageous for improving production performance. This general improvement was likely due to common apparent LoF mutations in *pykF* in these isolates. Although *pykF* was one of the culturing-condition adaptation genes, albeit with low occurrence across these replicate control condition ALEs, a sole *pykF* deletion largely improved tolerance to isobutyrate (Fig. S5g). Mutations in *pykF* have commonly been seen in *E. coli* ALE experiments (Phaneuf et al., 2021; Wang et al., 2018) and a *pykF* deletion has also been shown to allow for increased production of many metabolites (Harder et al., 2016; Sengupta et al., 2015) by redirecting fluxes towards central carbon metabolism and reducing intracellular pyruvate levels (Al Zaid Siddiquee et al., 2004). Among these strains, the best producers were IBUA8-3 and IBUA8-10, isolated from the same ALE lineage. Compared to other isolates, these strains have N-terminal mutations in either IlvN (N17H) or IlvH (L9F), encoding acetolactate synthase I or III, respectively. Both genes are responsible for the first biosynthesis step for branched chain amino acids (i.e., L-valine, L-isoleucine, L-leucine) from pyruvate (Fig. 6a). It was reported that the N-termini of acetolactate synthases are important for feedback inhibition by L-valine (Kaplun et al., 2006; Mendel et al., 2001). Indeed, introducing the IlvH-L9F mutation into MG1655 substantially reduced growth inhibition in the presence of 5 g/L L-valine, although the effect was absent when only IBUA was present (Figs. S9a and S9b). Furthermore, reverting the L9F mutation to the wildtype sequence in IBUA8-3 caused a growth diauxy with a lengthy plateau at low cell density when grown in the presence of 12.5 g/L isobutyrate (Fig. S9c), while growth of the reverted mutant was fully restored to that of IBUA8-3 with the additional presence of 1 g/L L-isoleucine (Fig. S9d). These results demonstrate a growth auxotrophy for L-isoleucine in the presence of high levels of IBUA as a dominant mode of toxicity, and the mechanism by which IBUA8-3 and IBUA8-1 evolved to bypass this may be particularly compatible with enabling high levels of endogenous isobutyrate production. More details are provided in **Supplementary Note 2**.

We also introduced a 23BD production pathway (Xu et al., 2014) into MG1655 and 20 ALE-derived isolates by expressing three heterologous genes (*budA*, *budB*, and *budC* from *Enterobacter cloacae* subsp. *dissolvens*

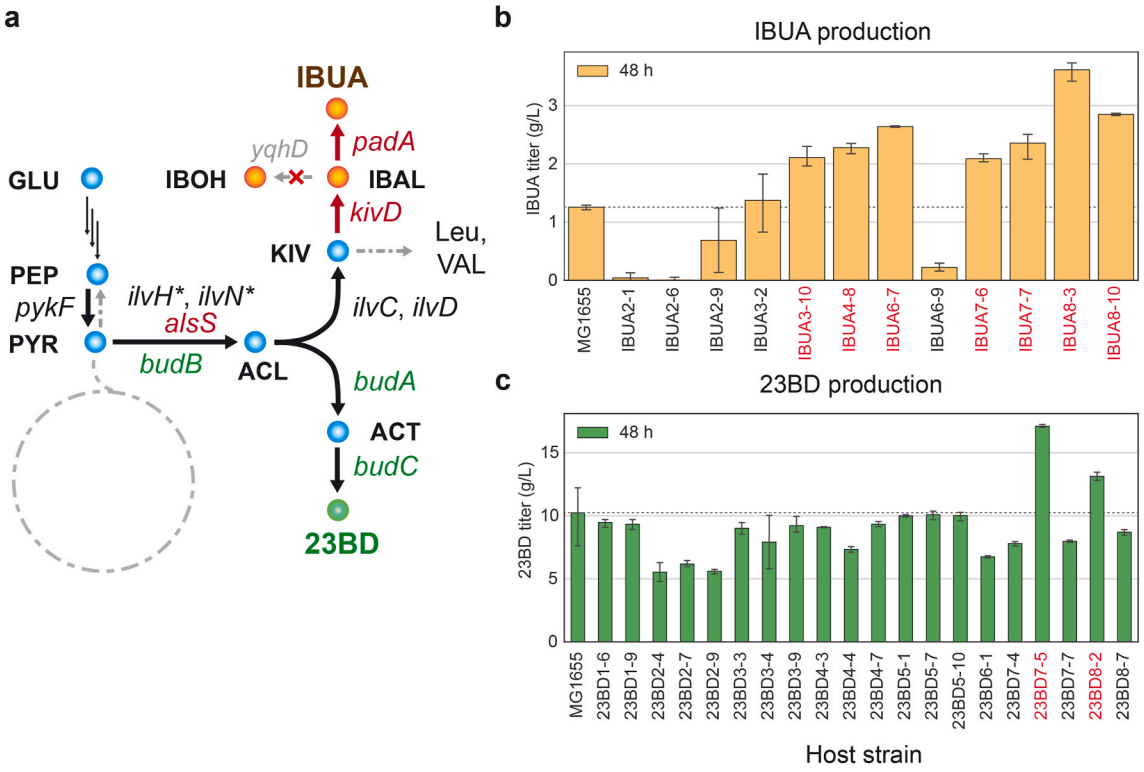

Fig. 6. Improved IBUA and 23BD production using ALE-derived tolerized strains
(**a**) Production pathways of IBUA and 23BD. IBUA can be produced by heterologous expression of *alsS* encoding an acetolactate synthase, *kidV* encoding a ketoisovalerate decarboxylase, and *padA* encoding phenylacetaldehyde dehydrogenase to generate isobutyrate from ketoisovalerate (KIV), with deletion of native *yqhD* to prevent production of isobutanol (IBOH). *E. coli* MG1655 also has native acetolactate synthase genes (*ilvI* and *ilvM* with regulatory subunits encoded by *ilvH and ilvN,* respectively). 23BD can be produced from pyruvate by heterologous expression of BudA, BudB, and BudC from *Enterobacter cloacae*. (**b**) IBUA titers of the engineered wildtype and isolates after 48 h. (**c**) 23BD titers of the engineered wildtype and isolates after 48 h. Error bars denote standard deviation of the titer for the corresponding strain (biological replicates $n = 4$). Strains that demonstrated improved production are colored in red. See Methods for detailed production conditions. Abbreviations: GLU, glucose; PEP, phophoenolpyruvate; PYR, pyruvate; ACL, acetolactate; KIV, ketoisovalerate; IBAL, isobutyrate; LEU, leucine; VAL, valine; IBOH, isobutanol; ACT, acetoin; 23BD, 2,3-butanediol. Heterologous genes and metabolites were colored in brown or green.

SDM) on a plasmid and deleting *hsdR* (a subunit of the EcoKI restriction system that targets a site in heterologous genes in the plasmid) in all isolates. Although all evolved clones did grow in minimal media, all engineered strains with the introduced pathway did not (data not shown) and required supplementation of yeast extract. There was also variation in 23BD production among the engineered ALE strains (Fig. 6c). However, two strains engineered from 23BD7-5 and 23BD8-2 showed a marked improvement in production of 23BD compared to the engineered reference strain. The 23BD7-5-based strain with the best titer had one unique mutation compared to two other strains from the same population (Table S2): a frameshift (Δ2 bp) in the *acrB* gene encoding a subunit of the AcrAB-TolC multidrug efflux pump. Deletion of *acrB* alone increased tolerance to 23BD (Fig. S4b). Similarly, it was reported that the inactivation of *acrA/acrB* improved isobutanol tolerance (Atsumi et al., 2010). 23BD8-2 was also unique in being the only 23BD isolate that did not possess a mutation in *metJ* (for which LoF by deletion was found to be beneficial for 23BD tolerance, Fig. S4b), further demonstrating the power of screening production in multiple isolates from many parallel populations, as some mutations beneficial for tolerance may counteract the ability to efficiently produce the compound endogenously. Overall, the superior production by the tolerant strains show that the reduced viability by high chemical concentration is a key rate limiting factor and the use of chemical-tolerant ALE isolates can improve endogenous production performance.

4. Conclusion

This study demonstrated that ALE can be used to increase the tolerance of microbial cells to a broad set of the commonly used industrial chemicals. Concentrations that allowed robust growth of *E. coli* (growth rate >0.2 h^{-1}) increased to levels of 60–400% from the initial concentration. Large percentage increases were observed for chemicals that initially were more toxic to *E. coli* (e.g., 400% in coumarate concentration, from 4 g/L to 20 g/L), while percent increases in concentrations of compounds that were initially less toxic, such as 12PD (60%, from 52 g/L to 83 g/L), were more modest. These levels of increase outline an expected range for additional chemicals using an ALE approach, and should translate to additional microorganisms (Mohedano et al., 2022; Van Dien, 2013; Wehrs et al., 2019). The systematic approach used here enabled direct comparisons of the evolvability of *E. coli* tolerance towards different chemical stresses on a significant scale.

To unveil tolerance mechanisms, we investigated convergent target genes that were mutated across conditions or a chemical/class-specific condition by analyzing a large sequencing dataset of 223 tolerized isolates. With the cutoff value of four as an independent occurrence of mutation, we identified 36 commonly mutated genes where 30 genes appeared to be directly associated with tolerance (Figs. 2 and 3). Most of the 36 genes had been previously relatively well-characterized and only two genes were less characterized (i.e., y-genes; *yeaR*, *yobF*) (Gao et al., 2018, 2021). In many conditions, we observed LoF mutations in membrane-related genes, especially those encoding transporters. For diacids, it was determined that cells were tolerized by inactivating an importer with promiscuous substrate specificities (Kell et al., 2015; Khersonsky and Tawfik, 2010; Lim et al., 2021; Radi et al., 2022). In addition, we found multiple commonly mutated genes related to

transcription/translation machineries, stress signaling pathways, and chemical-specific metabolism. Cross-comparison of tolerance to each chemical and NaCl showed that global tolerance was correlated to tolerance to a high-osmotic condition (Fig. 5d). This osmotolerance is particularly important for acidic/basic chemicals, which require neutralization, and thereby the addition of counterions, during fermentation-based production from pH-sensitive hosts (Wu et al., 2014). Additionally, the cross-chemical tolerance comparison and examination under no-stress conditions quantifies synergies and tradeoffs which can be further pursued in drill-down studies to understand the importance of such mutations (Sastry et al., 2019; Utrilla et al., 2016).

Lastly, we demonstrated the usefulness of tolerized strains by revealing the improved production of two chemicals, IBUA and 23BD. These two case studies allowed us to understand the effects of changes in common or strain-specific mutated genes on endogenous production as opposed to exogenous addition of these chemicals. Furthermore, a less frequent mutation can also improve production, which implies the necessity to characterize multiple strains, ideally isolated from independent lineages.

Collectively, our study unveiled, on a significant scale, diverse tolerance mechanisms in *E. coli* to the 11 targeted biochemicals. The generated comprehensive mutation dataset is accessible on ALEdb, which can be efficiently utilized to design bioproduction strains and understand mutational mechanisms.

Significance statement

Tolerance is a fundamental physiological property for microorganisms and is critical towards achieving efficient chemical bioproduction. However, the general understanding and rational design of host tolerance is challenged due to a limited understanding of tolerance mechanisms. Here we report a large mutation dataset and associated tolerance mechanisms identified in 223 *Escherichia coli* isolates tolerized to 11 industry-relevant chemicals via high-throughput adaptive laboratory evolution. We show that mutations frequently target particular subsystems, that osmotic stress plays an important role in stress phenotypes, and demonstrate significantly improved biochemical production by introducing a production pathway to genetically distinctive evolved isolates. The generated mutation dataset and uncovered tolerance mechanisms should be informative towards understanding tolerance phenotypes generally and broadly applicable towards developing efficient cell factories.

Author statement

Rebecca M. Lennen: Investigation, Methodology, Data Curation, Writing - Original Draft. Hyun Gyu Lim: Investigation, Methodology, Software, Data Curation, Writing - Original Draft. Kristian Jensen: Software, Methodology, Data Curation, Writing - Original Draft. Elsayed T. Mohammed: Investigation, Data CurationPatrick V. Phaneuf: Software, Data Curation. Myung Hyun Noh: Data Curation. Sailesh Malla: Investigation, Data Curation. Rosa A. Börner: Investigation, Data Curation. Ksenia Chekina: Investigation, Data CurationEmre Özdemir: Software, Data Curation. Ida Bonde: Software, Data Curation. Anna Koza: Investigation. Jérôme Maury: Investigation. Lasse E. Pedersen: Software, Data CurationLars Y. Schöning: Software, Data Curation. Nikolaus Sonnenschein: Software, Data Curation. Bernhard O. Palsson: Conceptualization, Writing - Review & Editing. Alex T. Nielsen: ConceptualizationMorten O.A. Sommer: Conceptualization. Markus J. Herrgård: Writing - Review & Editing, Supervision. Adam M. Feist: Writing - Review & Editing, Supervision.

Declaration of competing interest

All authors declare no competing interests.

Data availability

All data and source codes were uploaded to a public repository.

Acknowledgements

The authors acknowledge funding from the Novo Nordisk Foundation (Grant numbers NNF10CC1016517 and NNF140C0011269). Myung Hyun Noh appreciates funding from the National Research Foundation (NRF) of Korea (NRF-2021R1A6A3A03043982). The authors thank Prof. Katy C. Kao at San Jose State University and Prof. Hannes Link at University of Tübingen in Germany for fruitful discussions. A part of Fig. 3 was prepared by using images downloaded from images from BioRender (https://BioRender.com) with an academic license.

Appendix A. Supplementary data

Supplementary data to this article can be found online at https://doi.org/10.1016/j.ymben.2023.01.012.

References

Al Zaid Siddiquee, K., Arauzo-Bravo, M.J., Shimizu, K., 2004. Metabolic flux analysis of pykF gene knockout Escherichia coli based on 13C-labeling experiments together with measurements of enzyme activities and intracellular metabolite concentrations. Appl. Microbiol. Biotechnol. 63, 407–417. https://doi.org/10.1007/s00253-003-1357-9.

Alper, H., Moxley, J., Nevoigt, E., Fink, G.R., Stephanopoulos, G., 2006. Engineering yeast transcription machinery for improved ethanol tolerance and production. Science 314, 1565–1568. https://doi.org/10.1126/science.1131969.

Anand, A., Chen, K., Catoiu, E., Sastry, A.V., Olson, C.A., Sandberg, T.E., Seif, Y., Xu, S., Szubin, R., Yang, L., Feist, A.M., Palsson, B.O., 2020. OxyR is a convergent target for mutations acquired during adaptation to oxidative stress-prone metabolic states. Mol. Biol. Evol. 37, 660–667. https://doi.org/10.1093/molbev/msz251.

Anand, A., Chen, K., Yang, L., Sastry, A.V., Olson, C.A., Poudel, S., Seif, Y., Hefner, Y., Phaneuf, P.V., Xu, S., Szubin, R., Feist, A.M., Palsson, B.O., 2019. Adaptive evolution reveals a tradeoff between growth rate and oxidative stress during naphthoquinone-based aerobic respiration. Proc. Natl. Acad. Sci. U.S.A. 116, 25287–25292. https://doi.org/10.1073/pnas.1909987116.

Atsumi, S., Wu, T.-Y., Machado, I.M.P., Huang, W.-C., Chen, P.-Y., Pellegrini, M., Liao, J. C., 2010. Evolution, genomic analysis, and reconstruction of isobutanol tolerance in Escherichia coli. Mol. Syst. Biol. 6, 449. https://doi.org/10.1038/msb.2010.98.

Chen, Y., Boggess, E.E., Ocasio, E.R., Warner, A., Kerns, L., Drapal, V., Gossling, C., Ross, W., Gourse, R.L., Shao, Z., Dickerson, J., Mansell, T.J., Jarboe, L.R., 2020. Reverse engineering of fatty acid-tolerant Escherichia coli identifies design strategies for robust microbial cell factories. Metab. Eng. 61, 120–130. https://doi.org/10.1016/j.ymben.2020.05.001.

Conrad, T.M., Frazier, M., Joyce, A.R., Cho, B.-K., Knight, E.M., Lewis, N.E., Landick, R., Palsson, B.Ø., 2010. RNA polymerase mutants found through adaptive evolution reprogram *Escherichia coli* for optimal growth in minimal media. Proc. Natl. Acad. Sci. U.S.A. 107, 20500–20505. https://doi.org/10.1073/pnas.0911253107.

Datta, S., Costantino, N., Court, D.L., 2006. A set of recombineering plasmids for gram-negative bacteria. Gene 379, 109–115. https://doi.org/10.1016/j.gene.2006.04.018.

Deatherage, D.E., Barrick, J.E., 2014. Identification of mutations in laboratory-evolved microbes from next-generation sequencing data using breseq. In: Sun, L., Shou, W. (Eds.), Engineering and Analyzing Multicellular Systems: Methods and Protocols. Springer New York, New York, NY, pp. 165–188. https://doi.org/10.1007/978-1-4939-0554-6_12.

Deparis, Q., Claes, A., Foulquié-Moreno, M.R., Thevelein, J.M., 2017. Engineering tolerance to industrially relevant stress factors in yeast cell factories. FEMS Yeast Res. 17 https://doi.org/10.1093/femsyr/fox036.

Du, B., Olson, C.A., Sastry, A.V., Fang, X., Phaneuf, P.V., Chen, K., Wu, M., Szubin, R., Xu, S., Gao, Y., Hefner, Y., Feist, A.M., Palsson, B.O., 2020. Adaptive laboratory evolution of Escherichia coli under acid stress. Microbiology 166, 141–148. https://doi.org/10.1099/mic.0.000867.

Erian, A.M., Gibisch, M., Pflügl, S., 2018. Engineered E. coli W enables efficient 2,3-butanediol production from glucose and sugar beet molasses using defined minimal medium as economic basis. Microb. Cell Factories 17, 190. https://doi.org/10.1186/s12934-018-1038-0.

Fedorchuk, T.P., Khusnutdinova, A.N., Evdokimova, E., Flick, R., Di Leo, R., Stogios, P., Savchenko, A., Yakunin, A.F., 2020. One-pot biocatalytic transformation of adipic acid to 6-aminocaproic acid and 1,6-hexamethylenediamine using carboxylic acid reductases and transaminases. J. Am. Chem. Soc. 142, 1038–1048. https://doi.org/10.1021/jacs.9b11761.

Gao, Y., Lim, H.G., Verkler, H., Szubin, R., Quach, D., Rodionova, I., Chen, K., Yurkovich, J.T., Cho, B.-K., Palsson, B.O., 2021. Unraveling the functions of

uncharacterized transcription factors in Escherichia coli using ChIP-exo. Nucleic Acids Res. 49, 9696–9710. https://doi.org/10.1093/nar/gkab735.
Gao, Y., Yurkovich, J.T., Seo, S.W., Kabimoldayev, I., Dräger, A., Chen, K., Sastry, A.V., Fang, X., Mih, N., Yang, L., Eichner, J., Cho, B.-K., Kim, D., Palsson, B.O., 2018. Systematic discovery of uncharacterized transcription factors in Escherichia coli K-12 MG1655. Nucleic Acids Res 46, 10682–10696. https://doi.org/10.1093/nar/gky752.
Harden, M.M., He, A., Creamer, K., Clark, M.W., Hamdallah, I., Martinez 2nd, K.A., Kresslein, R.L., Bush, S.P., Slonczewski, J.L., 2015. Acid-adapted strains of Escherichia coli K-12 obtained by experimental evolution. Appl. Environ. Microbiol 81, 1932–1941. https://doi.org/10.1128/AEM.03494-14.
Harder, B.-J., Bettenbrock, K., Klamt, S., 2016. Model-based metabolic engineering enables high yield itaconic acid production by Escherichia coli. Metab. Eng. 38, 29–37. https://doi.org/10.1016/j.ymben.2016.05.008.
Henritzi, S., Fischer, M., Grininger, M., Oreb, M., Boles, E., 2018. An engineered fatty acid synthase combined with a carboxylic acid reductase enables de novo production of 1-octanol in Saccharomyces cerevisiae. Biotechnol. Biofuels 11, 150. https://doi.org/10.1186/s13068-018-1149-1.
Horinouchi, T., Suzuki, S., Kotani, H., Tanabe, K., Sakata, N., Shimizu, H., Furusawa, C., 2017. Prediction of cross-resistance and collateral sensitivity by gene expression profiles and genomic mutations. Sci. Rep. 7, 14009 https://doi.org/10.1038/s41598-017-14335-7.
Horst, J.P., Wu, T.H., Marinus, M.G., 1999. Escherichia coli mutator genes. Trends Microbiol 7, 29–36. https://doi.org/10.1016/s0966-842x(98)01424-3.
Jendresen, C.B., Stahlhut, S.G., Li, M., Gaspar, P., Siedler, S., Förster, J., Maury, J., Borodina, I., Nielsen, A.T., 2015. Highly active and specific tyrosine ammonia-lyases from diverse origins enable enhanced production of aromatic compounds in bacteria and Saccharomyces cerevisiae. Appl. Environ. Microbiol. 81, 4458–4476. https://doi.org/10.1128/AEM.00405-15.
Jensen, K.F., 1993. The Escherichia coli K-12 “wild types” W3110 and MG1655 have an rph frameshift mutation that leads to pyrimidine starvation due to low pyrE expression levels. J. Bacteriol. 175, 3401–3407. https://doi.org/10.1128/jb.175.11.3401-3407.1993.
Kaplun, A., Vyazmensky, M., Zherdev, Y., Belenky, I., Slutzker, A., Mendel, S., Barak, Z., Chipman, D.M., Shaanan, B., 2006. Structure of the regulatory subunit of acetohydroxyacid synthase isozyme III from Escherichia coli. J. Mol. Biol. 357, 951–963. https://doi.org/10.1016/j.jmb.2005.12.077.
Kell, D.B., Swainston, N., Pir, P., Oliver, S.G., 2015. Membrane transporter engineering in industrial biotechnology and whole cell biocatalysis. Trends Biotechnol 33, 237–246. https://doi.org/10.1016/j.tibtech.2015.02.001.
Khersonsky, O., Tawfik, D.S., 2010. Enzyme promiscuity: a mechanistic and evolutionary perspective. Annu. Rev. Biochem. 79, 471–505. https://doi.org/10.1146/annurev-biochem-030409-143718.
Kildegaard, K.R., Hallström, B.M., Blicher, T.H., Sonnenschein, N., Jensen, N.B., Sherstyk, S., Harrison, S.J., Maury, J., Herrgård, M.J., Juncker, A.S., Forster, J., Nielsen, J., Borodina, I., 2014. Evolution reveals a glutathione-dependent mechanism of 3-hydroxypropionic acid tolerance. Metabolic Engineering. https://doi.org/10.1016/j.ymben.2014.09.004.
Kim, S., Jin, S.H., Lim, H.G., Lee, B., Kim, J., Yang, J., Seo, S.W., Lee, C.-S., Jung, G.Y., 2021. Synthetic cellular communication-based screening for strains with improved 3-hydroxypropionic acid secretion. Lab Chip 21, 4455–4463. https://doi.org/10.1039/d1lc00676b.
LaCroix, R.A., Palsson, B.O., Feist, A.M., 2017. A model for designing adaptive laboratory evolution experiments. Appl. Environ. Microbiol. 83 https://doi.org/10.1128/AEM.03115-16.
LaCroix, R.A., Sandberg, T.E., O’Brien, E.J., Utrilla, J., Ebrahim, A., Guzman, G.I., Szubin, R., Palsson, B.O., Feist, A.M., 2015. Use of adaptive laboratory evolution to discover key mutations enabling rapid growth of Escherichia coli K-12 MG1655 on glucose minimal medium. Appl. Environ. Microbiol. 81, 17–30. https://doi.org/10.1128/AEM.02246-14.
Lennen, R.M., Herrgård, M.J., 2014. Combinatorial strategies for improving multiple-stress resistance in industrially relevant Escherichia coli strains. Appl. Environ. Microbiol. 80, 6223–6242. https://doi.org/10.1128/AEM.01542-14.
Lennen, R.M., Kruziki, M.A., Kumar, K., Zinkel, R.A., Burnum, K.E., Lipton, M.S., Hoover, S.W., Ranatunga, D.R., Wittkopp, T.M., Marner 2nd, W.D., Pfleger, B.F., 2011. Membrane stresses induced by overproduction of free fatty acids in Escherichia coli. Appl. Environ. Microbiol. 77, 8114–8128. https://doi.org/10.1128/AEM.05421-11.
Lennen, R.M., Nilsson Wallin, A.I., Pedersen, M., Bonde, M., Luo, H., Herrgård, M.J., Sommer, M.O.A., 2016. Transient overexpression of DNA adenine methylase enables efficient and mobile genome engineering with reduced off-target effects. Nucleic Acids Res 44, e36. https://doi.org/10.1093/nar/gkv1090.
Lim, H.G., Eng, T., Banerjee, D., Alarcon, G., Lau, A.K., Park, M.-R., Simmons, B.A., Palsson, B.O., Singer, S.W., Mukhopadhyay, A., Feist, A.M., 2021. Generation of Pseudomonas putida KT2440 strains with efficient utilization of xylose and galactose via adaptive laboratory evolution. ACS Sustainable Chem. Eng. 9, 11512–11523. https://doi.org/10.1021/acssuschemeng.1c03765.
Lim, H.G., Fong, B., Alarcon, G., Magurudeniya, H.D., Eng, T., Szubin, R., Olson, C.A., Palsson, B.O., Gladden, J.M., Simmons, B.A., Mukhopadhyay, A., Singer, S.W., Feist, A.M., 2020. Generation of ionic liquid tolerant Pseudomonas putida KT2440 strains via adaptive laboratory evolution. Green Chem 22, 5677–5690. https://doi.org/10.1039/D0GC01663B.
Lim, H.G., Lim, J.H., Jung, G.Y., 2015. Modular design of metabolic network for robust production of n-butanol from galactose-glucose mixtures. Biotechnol. Biofuels 8, 137. https://doi.org/10.1186/s13068-015-0327-7.
Mans, R., Daran, J.-M.G., Pronk, J.T., 2018. Under pressure: evolutionary engineering of yeast strains for improved performance in fuels and chemicals production. Curr. Opin. Biotechnol. 50, 47–56. https://doi.org/10.1016/j.copbio.2017.10.011.
McCloskey, D., Xu, S., Sandberg, T.E., Brunk, E., Hefner, Y., Szubin, R., Feist, A.M., Palsson, B.O., 2018. Evolution of gene knockout strains of E. coli reveal regulatory architectures governed by metabolism. Nat. Commun. 9, 3796. https://doi.org/10.1038/s41467-018-06219-9.
Mendel, S., Elkayam, T., Sella, C., Vinogradov, V., Vyazmensky, M., Chipman, D.M., Barak, Z., 2001. Acetohydroxyacid synthase: a proposed structure for regulatory subunits supported by evidence from mutagenesis. J. Mol. Biol. 307, 465–477. https://doi.org/10.1006/jmbi.2000.4413.
Mohedano, M.T., Konzock, O., Chen, Y., 2022. Strategies to increase tolerance and robustness of industrial microorganisms. Synth Syst Biotechnol 7, 533–540. https://doi.org/10.1016/j.synbio.2021.12.009.
Mukhopadhyay, A., 2015. Tolerance engineering in bacteria for the production of advanced biofuels and chemicals. Trends Microbiol 23, 498–508. https://doi.org/10.1016/j.tim.2015.04.008.
Mundhada, H., Seoane, J.M., Schneider, K., Koza, A., Christensen, H.B., Klein, T., Phaneuf, P.V., Herrgard, M., Feist, A.M., Nielsen, A.T., 2017. Increased production of L-serine in Escherichia coli through adaptive laboratory evolution. Metab. Eng. 39, 141–150. https://doi.org/10.1016/j.ymben.2016.11.008.
Nguyen-Vo, T.P., Liang, Y., Sankaranarayanan, M., Seol, E., Chun, A.Y., Ashok, S., Chauhan, A.S., Kim, J.R., Park, S., 2019. Development of 3-hydroxypropionic-acid-tolerant strain of Escherichia coli W and role of minor global regulator yieP. Metab. Eng. 53, 48–58. https://doi.org/10.1016/j.ymben.2019.02.001.
Niu, W., Kramer, L., Mueller, J., Liu, K., Guo, J., 2019. Metabolic engineering of Escherichia coli for the de novo stereospecific biosynthesis of 1,2-propanediol through lactic acid. Metab Eng Commun 8, e00082. https://doi.org/10.1016/j.mec.2018.e00082.
Noh, M., Yoo, S.M., Kim, W.J., Lee, S.Y., 2017. Gene expression knockdown by modulating synthetic small RNA expression in Escherichia coli. Cell Syst 5, 418–426. e4. https://doi.org/10.1016/j.cels.2017.08.016.
Nyabako, B.A., Fang, H., Cui, F., Liu, K., Tao, T., Zan, X., Sun, W., 2020. Enhanced acid tolerance in lactobacillus acidophilus by atmospheric and room temperature plasma (ARTP) coupled with adaptive laboratory evolution (ALE). Appl. Biochem. Biotechnol. 191, 1499–1514. https://doi.org/10.1007/s12010-020-03264-3.
Park, S.J., Kim, E.Y., Noh, W., Park, H.M., Oh, Y.H., Lee, S.H., Song, B.K., Jegal, J., Lee, S. Y., 2013. Metabolic engineering of Escherichia coli for the production of 5-amino-valerate and glutarate as C5 platform chemicals. Metab. Eng. 16, 42–47. https://doi.org/10.1016/j.ymben.2012.11.011.
Peng, F., Widmann, S., Wünsche, A., Duan, K., Donovan, K.A., Dobson, R.C.J., Lenski, R. E., Cooper, T.F., 2018. Effects of beneficial mutations in pykF gene vary over time and across replicate populations in a long-term experiment with bacteria. Mol. Biol. Evol. 35, 202–210. https://doi.org/10.1093/molbev/msx279.
Pereira, R., Wei, Y., Mohamed, E., Radi, M., Malina, C., Herrgård, M.J., Feist, A.M., Nielsen, J., Chen, Y., 2019. Adaptive laboratory evolution of tolerance to dicarboxylic acids in Saccharomyces cerevisiae. Metab. Eng. 56, 130–141. https://doi.org/10.1016/j.ymben.2019.09.008.
Pham, H.L., Wong, A., Chua, N., Teo, W.S., Yew, W.S., Chang, M.W., 2017. Engineering a riboswitch-based genetic platform for the self-directed evolution of acid-tolerant phenotypes. Nat. Commun. 8, 411. https://doi.org/10.1038/s41467-017-00511-w.
Phaneuf, P.V., Gosting, D., Palsson, B.O., Feist, A.M., 2019. ALEdb 1.0: a database of mutations from adaptive laboratory evolution experimentation. Nucleic Acids Res 47, D1164–D1171. https://doi.org/10.1093/nar/gky983.
Phaneuf, P.V., Yurkovich, J.T., Heckmann, D., Wu, M., Sandberg, T.E., King, Z.A., Tan, J., Palsson, B.O., Feist, A.M., 2020. Causal mutations from adaptive laboratory evolution are outlined by multiple scales of genome annotations and condition-specificity. BMC Genomics 21, 514. https://doi.org/10.1186/s12864-020-06920-4.
Phaneuf, P.V., Zielinski, D.C., Yurkovich, J.T., Johnsen, J., Szubin, R., Yang, L., Kim, S. H., Schulz, S., Wu, M., Dalldorf, C., Ozdemir, E., Lennen, R.M., Palsson, B.O., Feist, A.M., 2021. Escherichia coli data-driven strain design using aggregated adaptive laboratory evolution mutational data. ACS Synth. Biol. 10, 3379–3395. https://doi.org/10.1021/acssynbio.1c00337.
Pontrelli, S., Fricke, R.C.B., Sakurai, S.S.M., Putri, S.P., Fitz-Gibbon, S., Chung, M., Wu, H.-Y., Chen, Y.-J., Pellegrini, M., Fukusaki, E., Liao, J.C., 2018. Directed strain evolution restructures metabolism for 1-butanol production in minimal media. Metab. Eng. 49, 153–163. https://doi.org/10.1016/j.ymben.2018.08.004.
Qi, Y., Liu, H., Chen, X., Liu, L., 2019. Engineering microbial membranes to increase stress tolerance of industrial strains. Metab. Eng. 53, 24–34. https://doi.org/10.1016/j.ymben.2018.12.010.
Qian, Z.-G., Xia, X.-X., Lee, S.Y., 2009. Metabolic engineering of Escherichia coli for the production of putrescine: a four carbon diamine. Biotechnol. Bioeng. 104, 651–662. https://doi.org/10.1002/bit.22502.
Radi, M.S., SalcedoSora, J.E., Kim, S.H., Sudarsan, S., Sastry, A.V., Kell, D.B., Herrgård, M.J., Feist, A.M., 2022. Membrane transporter identification and modulation via adaptive laboratory evolution. Metab. Eng. 72, 376–390. https://doi.org/10.1016/j.ymben.2022.05.004.
Reyes, L.H., Abdelaal, A.S., Kao, K.C., 2013. Genetic determinants for n-butanol tolerance in evolved Escherichia coli mutants: cross adaptation and antagonistic pleiotropy between n-butanol and other stressors. Appl. Environ. Microbiol. 79, 5313–5320. https://doi.org/10.1128/AEM.01703-13.
Reyes, L.H., Almario, M.P., Winkler, J., Orozco, M.M., Kao, K.C., 2012. Visualizing evolution in real time to determine the molecular mechanisms of n-butanol tolerance in Escherichia coli. Metab. Eng. 14, 579–590. https://doi.org/10.1016/j.ymben.2012.05.002.

Royce, L.A., Yoon, J.M., Chen, Y., Rickenbach, E., Shanks, J.V., Jarboe, L.R., 2015. Evolution for exogenous octanoic acid tolerance improves carboxylic acid production and membrane integrity. Metab. Eng. 29, 180–188. https://doi.org/10.1016/j.ymben.2015.03.014.

Sandberg, T.E., Salazar, M.J., Weng, L.L., Palsson, B.O., Feist, A.M., 2019. The emergence of adaptive laboratory evolution as an efficient tool for biological discovery and industrial biotechnology. Metab. Eng. 56, 1–16. https://doi.org/10.1016/j.ymben.2019.08.004.

Sastry, A.V., Gao, Y., Szubin, R., Hefner, Y., Xu, S., Kim, D., Choudhary, K.S., Yang, L., King, Z.A., Palsson, B.O., 2019. The Escherichia coli transcriptome mostly consists of independently regulated modules. Nat. Commun. 10, 5536. https://doi.org/10.1038/s41467-019-13483-w.

Sengupta, S., Jonnalagadda, S., Goonewardena, L., Juturu, V., 2015. Metabolic engineering of a novel muconic acid biosynthesis pathway via 4-hydroxybenzoic acid in Escherichia coli. Appl. Environ. Microbiol. 81, 8037–8043. https://doi.org/10.1128/AEM.01386-15.

Seo, S.W., Gao, Y., Kim, D., Szubin, R., Yang, J., Cho, B.-K., Palsson, B.O., 2017. Revealing genome-scale transcriptional regulatory landscape of OmpR highlights its expanded regulatory roles under osmotic stress in Escherichia coli K-12 MG1655. Sci. Rep. 7, 2181. https://doi.org/10.1038/s41598-017-02110-7.

Thorwall, S., Schwartz, C., Chartron, J.W., Wheeldon, I., 2020. Stress-tolerant non-conventional microbes enable next-generation chemical biosynthesis. Nat. Chem. Biol. 16, 113–121. https://doi.org/10.1038/s41589-019-0452-x.

Utrilla, J., O'Brien, E.J., Chen, K., McCloskey, D., Cheung, J., Wang, H., Armenta-Medina, D., Feist, A.M., Palsson, B.O., 2016. Global rebalancing of cellular resources by pleiotropic point mutations illustrates a multi-scale mechanism of adaptive evolution. Cell Syst 2, 260–271. https://doi.org/10.1016/j.cels.2016.04.003.

Van Dien, S., 2013. From the first drop to the first truckload: commercialization of microbial processes for renewable chemicals. Curr. Opin. Biotechnol. 24, 1061–1068. https://doi.org/10.1016/j.copbio.2013.03.002.

Volker, A.R., Gogerty, D.S., Bartholomay, C., Hennen-Bierwagen, T., Zhu, H., Bobik, T.A., 2014. Fermentative production of short-chain fatty acids in Escherichia coli. Microbiology 160, 1513–1522. https://doi.org/10.1099/mic.0.078329-0.

Wang, L.C., Morgan, L.K., Godakumbura, P., Kenney, L.J., Anand, G.S., 2012. The inner membrane histidine kinase EnvZ senses osmolality via helix-coil transitions in the cytoplasm. EMBO J 31, 2648–2659. https://doi.org/10.1038/emboj.2012.99.

Wang, X., Zorraquino, V., Kim, M., Tsoukalas, A., Tagkopoulos, I., 2018. Predicting the evolution of Escherichia coli by a data-driven approach. Nat. Commun. 9, 3562. https://doi.org/10.1038/s41467-018-05807-z.

Wehrs, M., Tanjore, D., Eng, T., Lievense, J., Pray, T.R., Mukhopadhyay, A., 2019. Engineering robust production microbes for large-scale cultivation. Trends Microbiol 27, 524–537. https://doi.org/10.1016/j.tim.2019.01.006.

Wu, W., Long, M.R., Zhang, X., Reed, J.L., Maravelias, C.T., 2018. A framework for the identification of promising bio-based chemicals. Biotechnol. Bioeng. 115, 2328–2340. https://doi.org/10.1002/bit.26779.

Wu, X., Altman, R., Eiteman, M.A., Altman, E., 2014. Adaptation of Escherichia coli to elevated sodium concentrations increases cation tolerance and enables greater lactic acid production. Appl. Environ. Microbiol. 80, 2880–2888. https://doi.org/10.1128/AEM.03804-13.

Wu, Y., Jameel, A., Xing, X.-H., Zhang, C., 2022. Advanced strategies and tools to facilitate and streamline microbial adaptive laboratory evolution. Trends Biotechnol 40, 38–59. https://doi.org/10.1016/j.tibtech.2021.04.002.

Xu, Y., Chu, H., Gao, C., Tao, F., Zhou, Z., Li, K., Li, L., Ma, C., Xu, P., 2014. Systematic metabolic engineering of Escherichia coli for high-yield production of fuel biochemical 2,3-butanediol. Metab. Eng. 23, 22–33. https://doi.org/10.1016/j.ymben.2014.02.004.

Yang, Z., Zhang, Z., 2019. Recent advances on production of 2, 3-butanediol using engineered microbes. Biotechnol. Adv. 37, 569–578. https://doi.org/10.1016/j.biotechadv.2018.03.019.

Yomano, L.P., York, S.W., Ingram, L.O., 1998. Isolation and characterization of ethanol-tolerant mutants of Escherichia coli KO11 for fuel ethanol production. J. Ind. Microbiol. Biotechnol. 20, 132–138. https://doi.org/10.1038/sj.jim.2900496.

Zhang, K., Woodruff, A.P., Xiong, M., Zhou, J., Dhande, Y.K., 2011. A synthetic metabolic pathway for production of the platform chemical isobutyric acid. ChemSusChem 4, 1068–1070. https://doi.org/10.1002/cssc.201100045.

Zhao, M., Huang, D., Zhang, X., Koffas, M.A.G., Zhou, J., Deng, Y., 2018. Metabolic engineering of Escherichia coli for producing adipic acid through the reverse adipate-degradation pathway. Metab. Eng. 47, 254–262. https://doi.org/10.1016/j.ymben.2018.04.002.

Zorraquino, V., Kim, M., Rai, N., Tagkopoulos, I., 2017. The genetic and transcriptional basis of short and long term adaptation across multiple stresses in Escherichia coli. Mol. Biol. Evol. 34, 707–717. https://doi.org/10.1093/molbev/msw269.